ERDC TR-06-15

US Army Corps of Engineers®

System-Wide Water Resources Program
Submerged Aquatic Vegetation Restoration Research Program

Waves in Seagrass Systems: Review and Technical Recommendations

Evamaria W. Koch, Larry P. Sanford, Shih-Nan Chen,
Deborah J. Shafer, and Jane McKee Smith

November 2006

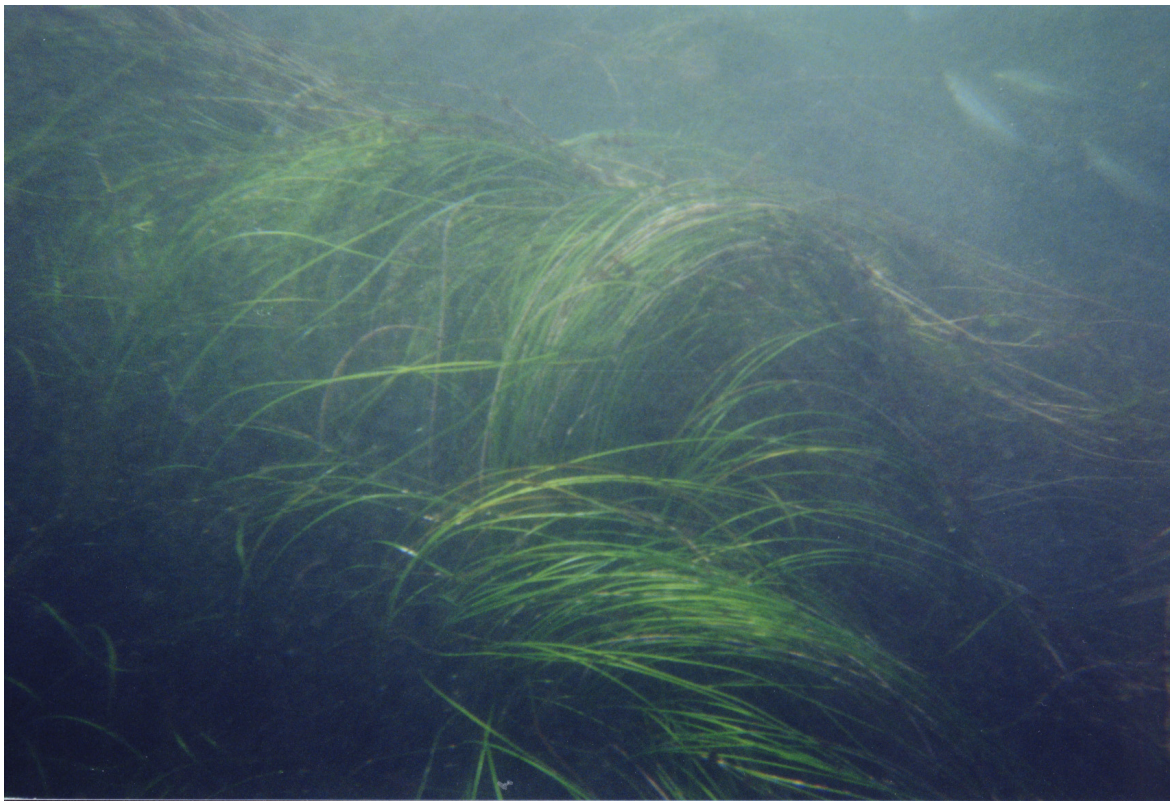

Engineer Research and Development Center

System-Wide Water Resources Research Program
and Submerged Aquatic Vegetation Restoration
Research Program

ERDC TR-06-15
November 2006

Waves in Seagrass Systems: Review and Technical Recommendations

Evamaria W. Koch, Larry P. Sanford, and Shih-Nan Chen

Horn Point Laboratory, University of Maryland Center for Environmental Science
P.O. Box 775
Cambridge, MD 21613

Deborah J. Shafer

Environmental Laboratory
U.S. Army Engineer Research and Development Center
3909 Halls Ferry Road
Vicksburg, MS 39180-6199

Jane McKee Smith

Coastal and Hydraulics Laboratory
U.S. Army Engineer Research and Development Center
3909 Halls Ferry Road
Vicksburg, MS 39180-6199

Final report

Prepared for U.S. Army Corps of Engineers
Washington, DC 20314-1000

Under Work Unit 122687

Abstract: Seagrasses are rooted flowering marine plants that provide a variety of ecosystem services to the coastal areas they colonize. Attenuation of currents and waves and sediment stabilization are often listed among these services. Although we have a reasonably good understanding of how currents affect seagrasses and vice-versa, less is known about interactions between waves and seagrasses, and standard methods for research on waves in seagrass systems have not yet been established. This report presents background information needed to inform and encourage further studies on waves in seagrass systems from both field and modeling perspectives. It reviews current knowledge of waves in seagrass systems, encompassing field and laboratory data as well as modeling efforts. It then describes various methods for measuring waves in seagrass colonized areas and modeling the dynamics of wave-seagrass interactions. Standardization of experimental designs, instrumentation, analyses, and modeling approaches to allow for ready comparison between studies is encouraged.

Contents

Figures and Tables

Figures

Tables

Preface

This report provides a review of waves in nearshore seagrass ecosystems. Understanding the interaction of seagrasses with waves, currents, and sediments is critical for maintaining and initiating seagrass beds in wave environments. This study was funded jointly through the System-Wide Water Resources Program (SWWRP), Wave Computations for Ecosystem Modeling Work Unit, and the Submerged Aquatic Vegetation Restoration Research (SAVRR) Program. Dr. Steven L. Ashby is the Program Manager of SWWRP and Deborah J. Shafer is the Program Manager of the SAVRR Program.

The authors would like to thank Dr. Mark Fonseca for his comments on an earlier version of the manuscript and the Integration and Application Network (ian.umces.edu) at the University of Maryland Center for Environmental Science for providing the symbols used in Figures 1 and 2.

This study was performed by Drs. Evamaria W. Koch, Larry P. Sandford, and Shih-Nan Chen, University of Maryland, Deborah J. Shafer, U.S. Army Engineer Research and Development Center (ERDC), Environmental Laboratory (EL), and Dr. Jane McKee Smith, ERDC, Coastal and Hydraulics Laboratory (CHL). This study was performed under the supervision of Ty V. Wamsley, Chief, Coastal Processes Branch, CHL, Bruce A. Ebersole, Chief, Flood and Storm Protection Division, CHL, Dr. William D. Martin, Deputy Director CHL, Thomas W. Richardson, Director, CHL, Dr. Morris Mauney, Chief, Wetland and Coastal Ecology Branch, EL, Dr. David Tazik, Chief, Ecosystem Evaluation and Engineering Division, EL, Dr. Mike Passmore, Acting Deputy Director, EL, and Dr. Beth Fleming, Director, EL.

COL Richard B. Jenkins was Commander and Executive Director of ERDC. Dr. James R. Houston was Director.

1 Introduction

Seagrasses and their fluid environment

Seagrasses are marine flowering plants. They differ from macroalgae (also known as seaweed) as these do not flower but reproduce via spores. Seagrasses also have a root and true rhizome system while macroalgae only have rhizoids. As a result, macroalgae tend to attach to hard substrates such as shell and rocks while most seagrasses colonize soft substrates such as sand. However, some seagrasses, such as those of the genus *Phyllospadix* and sometimes *Posidonia* attach to rocks and are exposed to relatively high wave energy. In contrast, seagrasses colonizing soft substrates are usually found in more quiescent (i.e., wave-sheltered) areas.

Seagrasses are found in coastal areas around the world except Antarctica (Green and Short 2003) and are limited in the depths and areas they colonize by light availability (Dennison et al. 1993) and physical and geological parameters (Koch 2001), respectively. Seagrasses require relatively high light levels (11 to 20 percent of surface light) (Dennison et al. 1993; Duarte 1991; Gallegos and Kenworthy 1996; Kenworthy and Fonseca 1996) when compared to other marine photosynthetic organisms such as phytoplankton, which only requires 1 percent surface light. As a result, seagrasses are generally found in shallow waters (< 90 m) (Duarte 1991) also influenced by waves. This can limit the geographical distribution of seagrasses as most species require relatively sheltered conditions to thrive (Fonseca and Bell 1998; Robbins and Bell 2000; Koch 2001). Excessively sheltered conditions such as those found in stagnant ponds or shoreward of breakwaters can also be detrimental to seagrasses (Koch 2001) and other organisms (Martin et al. 2005). An optimum balance between light availability and moderate wave climate is often found in estuaries, embayments, and coastal lagoons. Seagrasses are quite abundant in these areas. Adjacent animal communities and/or bathymetric features can also promote seagrass establishment via wave attenuation. For example, extensive seagrass beds are often found shoreward of coral reefs and sandbars where wave conditions are relatively quiescent (see review by Fonseca 1996).

The importance of seagrasses in coastal systems has been recognized since early settlers used their seeds as a food source and their leaves as insulation material (Wyllie-Echeverria et al. 2002). Although seagrasses are no

longer used for these purposes, their capacity to remove nutrients from the water column has recently been valued $19,000 /hectare/ year (Costanza et al. 1997). Other ecosystem services provided by seagrasses include serving as habitat for a variety of ecologically and economically valuable species, providing food to associated organisms directly (to turtles) and indirectly (via detritus and epiphytes), stabilizing the sediments they colonize, and sequestering carbon (Green and Short 2003).

Interactions between seagrasses and water flow

In their natural environment, seagrasses are exposed to wind-driven currents, tides, waves and wave-driven currents (Koch 2001). While these hydrodynamic processes affect seagrasses, seagrasses also affect these hydrodynamic processes. A feedback mechanism appears to develop between seagrasses and their fluid environment (Koch et al. 2006). For example, as a newly established seagrass bed attenuates currents and waves, fine and organic particles tend to be trapped increasing the nutrient availability to the plants (Kenworthy et al. 1982). As a result, seagrasses can grow faster and more robust (Short 1987). However, excessive attenuation of currents and waves by extremely dense seagrass beds or geomorphological features may lead to sediment organic contents so high that they become detrimental to seagrasses. Organic contents higher than 5 percent have been suggested as detrimental to seagrasses (Koch 2001; Kemp et al. 2004). Additionally, excessively weak currents and waves can also lead to limiting leaf diffusive boundary layer conditions (Fonseca and Kenworthy 1987). Currents below 5 cm/sec have been suggested as limiting to seagrasses due to a reduction in the flux of carbon and nutrients to the leaf surface (Koch 1994). In contrast, in areas with high wave exposure and strong currents, seagrass may be damaged due to excessive sediment transport, which does not allow seeds to become established, or eroding/burying existing seagrass beds. As a result, wave- or current-exposed areas tend to have patchy seagrasses or are unvegetated (Fonseca and Bell 1998; Hovel et al. 2002; Krause-Jensen et al. 2003), and an intermediate flow regime may be optimal for seagrass growth and development (Koch et al. 2006).

One of the most complex water flow systems is that in vegetated areas (Raupach et al. 1991, Finnigan 2000). Not only can water flow affect seagrasses and seagrasses affect water flow (as previously described) but seagrasses and water flow may interact in highly coupled, nonlinear ways. Kelvin-Helmholtz instabilities that generate large coherent vortices at the interface between the canopy and the overlaying water column lead to

wave-like oscillations referred to as monami (Ackerman and Okubo 1993). The vortices and the elastic and buoyant seagrass leaves interact causing the canopy to wave in a coherent manner. These vortices can penetrate into the canopy enhancing vertical transport between the water column and the canopy (Ghisalberti and Nepf 2002). As a result, recruitment of organisms (Grizzle et al. 1996), sediment dynamics and nutrient acquisition by the plants can be enhanced.

Due to the complexities of water flow in vegetated systems, hydrodynamics of seagrasses is a relatively unstudied field (Koch 2001). Although it is beginning to be understood how currents move through seagrass beds and how in turn seagrasses affect and are affected by currents (Koch et al. 2006), understanding about waves in seagrass systems is in its infancy (Fonseca and Cahalan 1992; Fonseca 1998).

The purpose of this publication is to provide engineers and scientists with the background information needed to encourage further studies of waves in seagrass systems from a field as well as a modeling perspective. Significant progress still needs to be made regarding how waves propagate through seagrass beds, how seagrasses stabilize the sediments they colonize and possibly also the adjacent shoreline, how much wave energy is tolerated by different seagrass species, and how much wave energy is beneficial for seagrass systems, just to cite a few. This report begins with a review the current knowledge of waves in seagrass systems including field and laboratory data as well as modeling efforts. Then methods are described that can be used to further study waves in seagrass colonized areas. It concludes with the latest models being developed to understand the dynamics between waves and seagrasses.

2 Background

Seagrass terminology

Although seagrass morphology closely resembles that of terrestrial grasses, botanically, seagrasses are more closely related to lilies than grasses. Seagrasses have a horizontal rhizome linking clusters of leaves referred to as shoots, and roots are usually found at each shoot (Figure 1). Seagrasses are true flowering plants. As a result, they also have flowers and seeds (Figure 1). The flowers of some species (e.g., *Halodule wrightii*, *Thalassia testudinum*) are found near the sediment surface while other seagrass species (e.g., *Zostera marina*, *Ruppia maritima*), when reproductive, form long vertical stems that can occupy most of or the entire water column. When most of the plant biomass, independent if in the form of reproductive or vegetative shoots, occupies a large portion of the water column, the vegetation is often referred to as a canopy (Figure 2). In contrast, when most of the seagrass biomass is found near the bottom, they are often referred to as meadows (Figure 2).

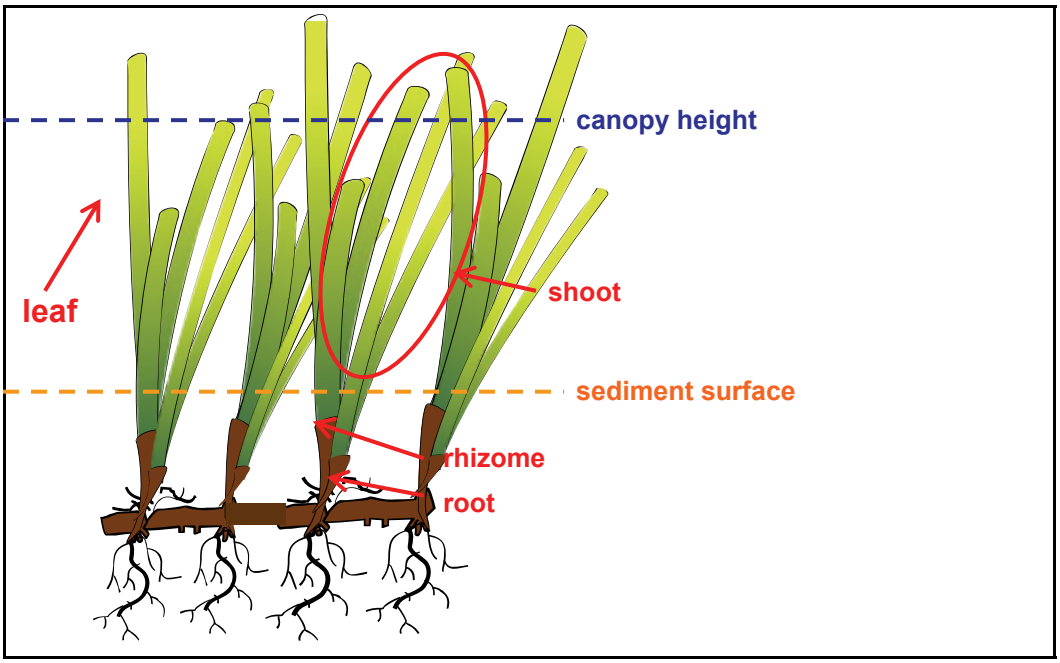

Figure 1. Nomenclature commonly used to describe parts of seagrasses and attributes of the canopy they form. Note that the leaves bend in the direction of currents and flap back and forth with waves. Therefore, the depicted canopy height is actually the maximum canopy height.

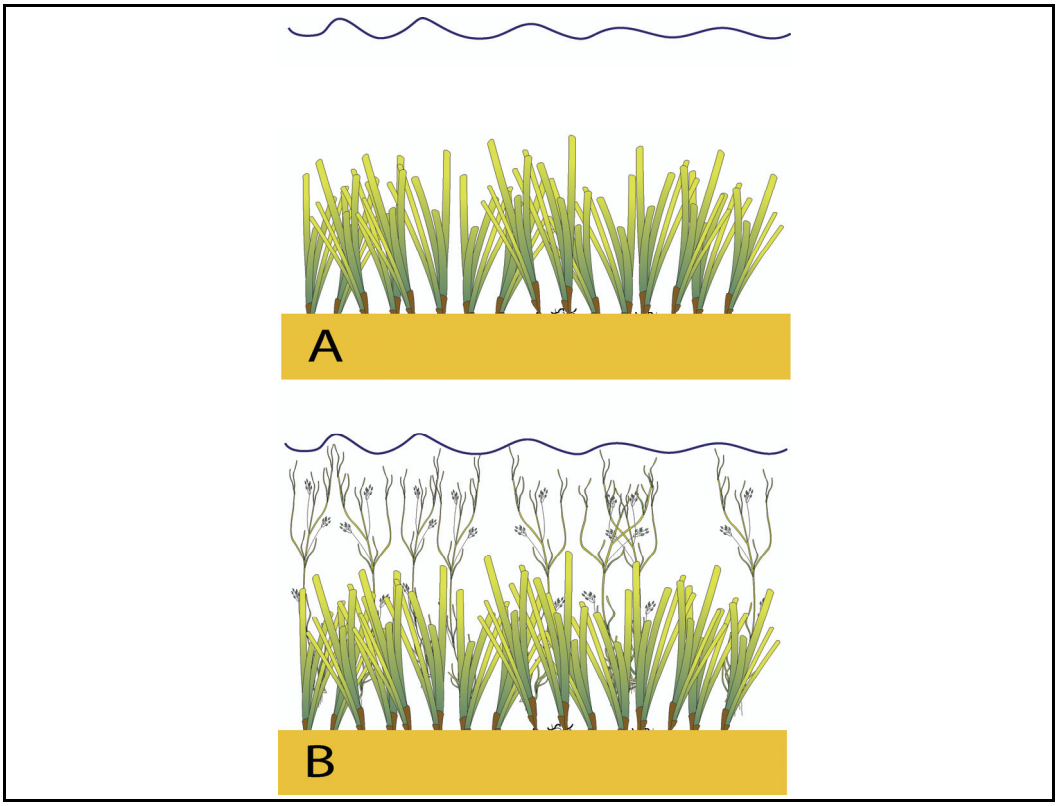

Figure 2. Diagram depicting the difference between a seagrass meadow (A) and seagrass canopy (B). Note that the meadow only occupies a small fraction of the water column while the canopy occupies the entire water column. In this case, the canopy is formed by the reproductive structures of a seagrass but often seagrass leaves can occupy the entire water column.

When quantifying the amount of seagrass present in an area, quite often the number of shoots in an area (e.g., 25 x 25 cm) is counted and expressed per m^2 (i.e., shoots/m^2). This leads to a parameter called "shoot density". This value varies between species. For example, a dense *Ruppia maritima* bed may have more than 3,000 shoots/m^2 while a dense *Zostera marina* bed may only have 2,000 shoots/m^2. This appears to be due to the biomass occupied by the leaves or leaf area (note that *Zostera* has wider leaves than *Ruppia*). Canopy height is also an important seagrass parameter when evaluating the impact of seagrasses on water flow. This parameter is usually obtained by averaging the tallest two-thirds of the leaves (Figure 1). The smallest seagrasses (genus *Halophila*) are only 2 or 3 cm tall while the largest seagrasses in the United States can reach 2 m in length (nonreproductive *Zostera marina* and *Phyllospadix* sp.). When reproductive, other seagrasses such as *Ruppia maritima* can also reach 1 m in length. Although canopy height measured in the form of the tallest leaves or reproductive structure is easy to quantify, it may not be a good

representation of the true canopy height observed in situ. When exposed to currents and waves, seagrass leaves tend to bend in the direction of the flow (Figure 3) leading to a canopy height smaller than the leaf or reproductive shoot length. Fonseca et al. (1982) described the angle of bending of *Zostera marina* shoots as a function of current velocity in a flume by the following equation:

$$Y = 62.8e^{-0.036u} \quad (1)$$

where Y is the bending angle measured from the horizontal and u is the current velocity in cm s^{-1}. Fonseca and Fisher (1986) also describe seagrass canopy compression (canopy height/water depth) as a function of Darcy's friction factor. Due to the complexity of modeling flexible structures in the aquatic environment, stiff cylinders are commonly considered in models (see Nepf 1999) which assume that canopy height equals leaf length. As seen from the Equation 1, this is an overestimation of canopy height and its effects on water flow.

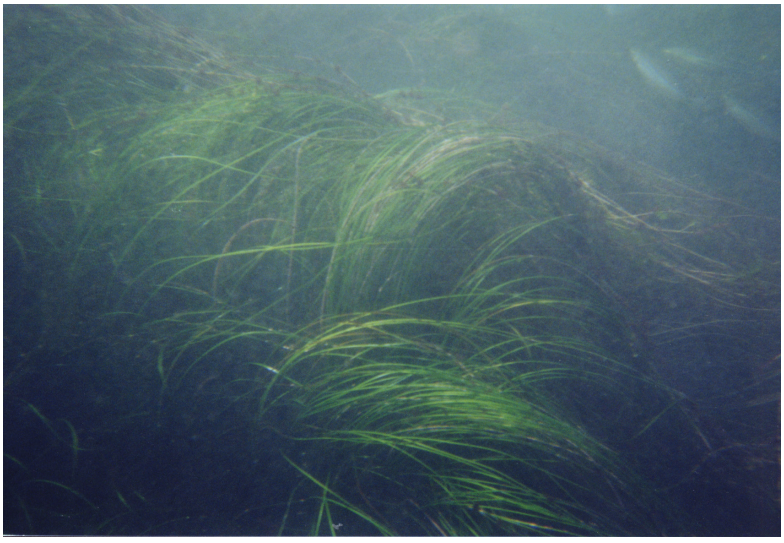

Figure 3. *Phyllospadix* swaying back and forth with the waves at a shallow site (2 to 3 m) in the Pacific Ocean, off Baja California, Mexico.

Nearshore waves: A brief summary of important characteristics

In the most general sense, a wave may be defined as a disturbance that travels in at least one spatial dimension through time, and to a good approximation transports energy without transporting mass. Waves that travel on the surface of the water are known as surface gravity waves; these are the waves that most directly affect nearshore seagrass beds. The waves

that are the main focus of this review are those that are generated (somewhere) by the wind and travel in the direction of the wind. Because the time and space scales of generation of these waves are long, they may be approximated mathematically by a continuous sine (or cosine) function, so the surface elevation η of a wave traveling over a distance *x* through time *t* can be expressed as:

$$\eta(x,t) = \frac{H}{2}\sin(\frac{2\pi x}{L} - \frac{2\pi t}{T}) \quad (2)$$

In Equation 2, *H* is defined as the local wave height, the vertical distance between a crest (the highest point of the wave) and the adjacent trough (the lowest point of the wave); Figure 4. *L* is defined as the wavelength of the wave, the distance between successive crests in the direction of wave travel. *T* is defined as the period of the wave, the time between the passage of two successive crests measured by a fixed observer. The phase speed (the speed at which a wave crest travels) is defined by $c=L/T$. Equation 2 is known as the linear or Airy wave approximation, and it is quite approximate for a wind sea as it approaches the shoreline. Real waves include variations in wave height, period, and direction, and deviate from the sinusoidal shape in shallow water. However, it is remarkable how well this expression and the relationships that result from it describe basic wave dynamics in the nearshore. Nearshore waves may also be generated by transient disturbances such as boating traffic (boat waves), or by interactions between breaking waves and the shoreline geometry (infragravity waves), but these wave types are not well described by Equation 2 so are not considered further here.

The most important aspect of wave dynamics is the transport of energy. The energy *E* of a wave averaged over a wave period is defined by:

$$E = \frac{1}{8}\rho g H^2 \quad (3)$$

where ρ is the density of water and *g* is the gravitational constant, in units of Joules (or Watt-sec) per unit of surface area. This energy is transported in the direction of wave propagation at the group velocity c_g of the wave, such that the rate of wave energy transport, also called the wave energy flux or wave power, is given by:

$$E_f = c_g E \tag{4}$$

in watts per unit of wave crest length.

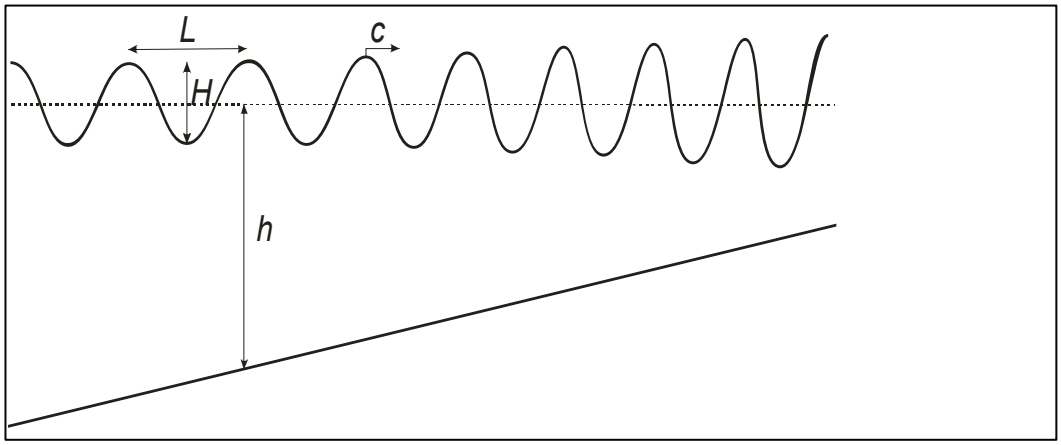

Figure 4. Schematic diagram of a shoaling wave as it approaches shore. Variable names are defined in the text. As the depth *h* becomes shallower nearshore, the speed of the wave decreases. The wave period cannot change, so in order for the speed to decrease the wavelength must decrease. The wave height must also increase to conserve wave power, unless dissipation is significant. The wave steepens as a result of both changes, and eventually breaks.

Note that c_g is not necessarily the same as the wave phase speed c shown in Figure 4. In general, the group velocity is given by:

$$c_g = \frac{1}{2}\left[1 + \frac{\frac{4\pi}{L}h}{\sinh\left(\frac{4\pi}{L}h\right)}\right] \tag{5}$$

where L is given by the solution of the transcendental function:

$$\left(\frac{2\pi}{T}\right)^2 = \frac{2\pi g}{L}\left(\tanh\frac{2\pi h}{L}\right) \tag{6}$$

For shallow-water waves with $h/L < 0.04$, where h is the water depth, the phase speed and group velocity are the same and depend only on water depth:

$$c_g = c = \sqrt{gh} \tag{7}$$

For deep water waves with $h/L > 0.5$:

$$c_g = \frac{1}{2}c = \frac{gT}{4\pi} \tag{8}$$

That is, the energy only travels half as fast as the individual waves and both depend only on the wave period. Between these limits, for transitional or intermediate waves, the expressions for c and c_g are complex functions of both depth and period (see e.g., Dean and Dalrymple 1991).

Figure 5 shows the group velocity c_g for wave periods and depths relevant for most nearshore seagrass beds. Clearly, the behavior of waves interacting with seagrass beds can vary significantly depending on the wave periods and depths of interest. Note that for long-period (e.g., T = 12 sec), shallow-water waves c_g changes rapidly as shore is approached. These waves are strongly affected by the local depth, produce strong near-bottom wave action, and are subject to significant steepening (through wave shoaling) and breaking. For short-period (e.g., T = 2 sec) waves c_g does not change much until the waves are in shallow water. These waves are only weakly affected by the local depth, produce weaker near-bottom wave action (for equivalent wave height), and experience much less steepening and breaking than the long-period waves in the same water depths. Waves interact with the bottom based on the relative water depth (h/L), so long-period waves have longer wavelengths and interact with the bottom at much deeper depths.

The waves of interest here are generated by the action of the wind stress on the surface of the water. Waves become longer and higher as the fetch and/or the duration increase. Fetch is the over-water distance in the direction of the wind, and duration is the amount of time the wind has been blowing from that direction. Waves generated in shallow water tend to be shorter and smaller than waves generated in deep water. Swells are long waves generated in deep water that outrun their source region, sometimes traveling thousands of kilometers before encountering land. They tend to be unidirectional (from a single direction), narrow banded (energy is concentrated in a narrow range of periods), and to travel in groups of larger waves. Waves generated by local winds, often referred to as chop or windsea, are more chaotic short waves with a broad spectrum of wave heights, periods, and directions centered on mean values that can change rapidly as the wind changes. Long-period waves (swells and seas) tend to domi-

nate nearshore environments with open ocean exposure, but short-period wind waves usually dominant in closed or semi-enclosed water bodies. Wave power, once generated, is either conserved or dissipated as a wave approaches shore and is transformed by interactions with the bottom slope, seagrass beds, or underwater obstacles such as breakwaters or offshore bars. At the shoreline, any remaining wave energy is either reflected back or dissipated by breaking. Violent dissipation of wave energy in the nearshore through breaking is responsible for the high rates of sediment transport and/or shoreline erosion that commonly occur along wave-exposed coasts.

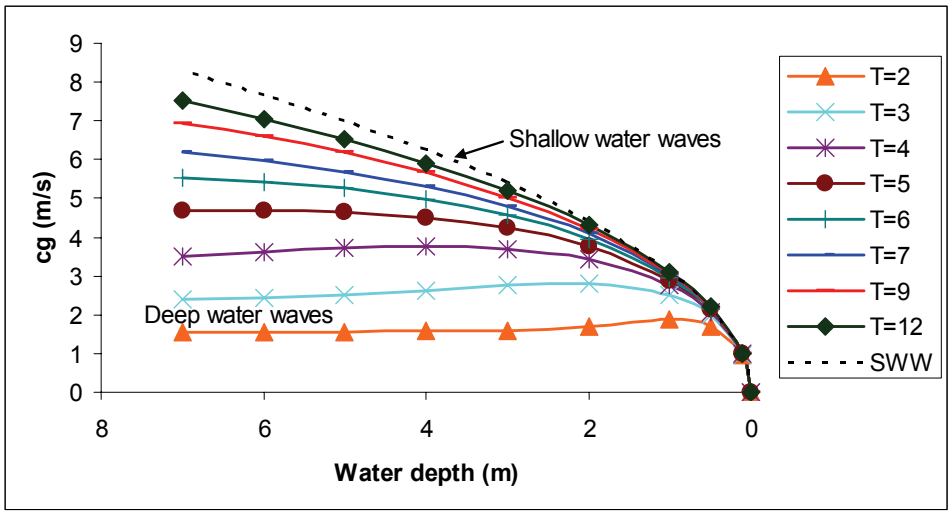

Figure 5. Group velocities predicted by linear wave theory for *T*=2-12 sec.

Wave transformation patterns are often complex near the shore, especially in the presence of complex bathymetry and/or shoreline geometry, or significant local changes in wave drag (Figure 6). Waves approaching the shoreline at an angle will bend toward the shoreline as the group velocity nearest the shore slows down; this process is known as refraction. Waves encountering an obstacle of limited length (a breakwater or seawall, for example) will be entirely or partially blocked by the obstacle, but wave energy will spread into the shadow of the obstacle from beyond its edges via diffraction. A marked local change in bottom roughness/drag, such as produced by an oyster reef or a seagrass bed, will have some of the same effects as a breakwater except that complete blocking of wave energy is replaced by more gradual energy dissipation. This allows more of the incident wave energy to continue propagating past the reef/bed than for a breakwater. In all cases, changes in wave height are determined by the requirement that the wave energy flux budget be balanced, such that the to-

tal energy flux between two wave rays (lines perpendicular to the crests in the direction of propagation) is either conserved or dissipated. The combination of all of these wave transformation effects as waves transition from deep to shallow water virtually mandates the use of a numerical model for anything more than the simplest of problems.

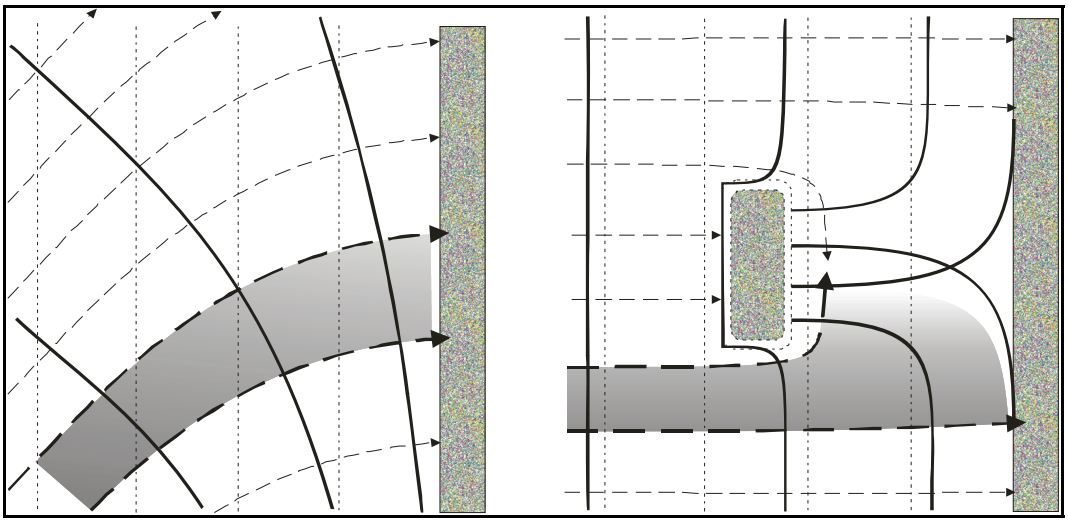

Figure 6. Illustrations of refraction (left panel) and diffraction (right panel). The solid lines represent the wave crests, the short dashed lines represent depth contours, and the long dashed lines represent wave rays. Turning and spreading of wave rays are apparent in both cases, resulting in a redirection and decrease of wave power. This decrease is most apparent in the shadow of the breakwater (right), where crossing of waves from different directions also leads to interference patterns.

3 How Seagrasses Affect Waves and Wave-Dependent Processes

Wave attenuation

Seagrasses tend to attenuate waves, especially in shallow waters where waves interact with the seagrass canopy the same way as shallow waves interact with the bottom. Even so, most waves in seagrass beds seem to be intermediary in nature (i.e., $0.04 < h/L < 0.5$). The degree of wave attenuation observed in a seagrass bed is directly related to the fraction of the water column occupied by the vegetation. Wave attenuation is highest when seagrasses occupy a large portion (>50 percent) of the water column (Ward et al. 1984; Fonseca and Cahalan 1992; Figure 7). A flume study measured wave attenuations between 20 and 76 percent over 1-m length when the plants were occupying the entire water depth (Fonseca and Cahalan 1992), whereas field studies measured values between 1.6 and 80 percent (Koch 1996; Prager and Halley 1999). This wide variation in field data appears to be related to tidal fluctuations, i.e. fraction of the water column occupied by the vegetation: at high tide, wave attenuation is smaller than at low tide (Figure 7). Reduction in wave energy is also observed in relatively deep beds exposed to long waves. For example, Verduin and Backhaus (2000) observed that 15-sec waves were attenuated by an *Amphibolis antarctica* bed at 5-m depth (note that $h/L = 0.33$, i.e., intermediate waves).

Flooding is usually associated with severe storm events. Therefore, it could be speculated that seagrass beds will be less effective in attenuating waves (canopy occupies a smaller fraction of the water column) when this ecosystem service is needed the most. However, storms also generate longer waves. Therefore, theoretically, seagrasses may still attenuate waves during storm events when flooding occurs. This complex relationship between storm waves, flooding, and seagrass-induced wave attenuation still needs to be verified.

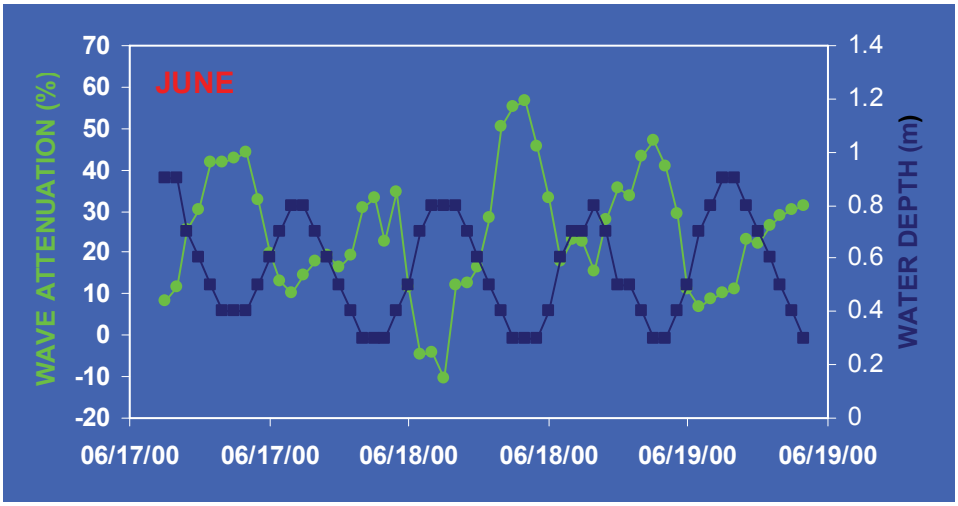

Figure 7. Wave attenuation in a dense (1,270 ± 92 shoots/m²) *Ruppia maritima* bed off Bishop's Head Point in Chesapeake Bay, MD. Note that wave attenuation is inversely related to water/tidal level.

Sediment stabilization

An ecosystem service commonly listed for seagrasses is sediment and shoreline stabilization. Seagrasses effectively reduce current velocities and attenuate waves (Fonseca et al. 1982; Fonseca and Fisher 1986; Gambi et al. 1990; Fonseca 1996; Koch 1996; Wallance and Cox 1997; Koch and Gust 1999; Verduin and Backhaus 2000; Peterson et al. 2004) and, as a result, sediment erosion is decreased and particle deposition is enhanced in seagrass beds. Consequently, sediments in vegetated areas are usually finer and more organic than in adjacent unvegetated areas (Kenworthy et al. 1982; Fonseca and Koehl 2006). Quiescent hydrodynamic conditions are likely to also contribute to the high recruitment of larvae and juvenile stages of many organisms such as crustaceans and fishes.

Due to their capacity to alter their environment, seagrasses have been referred to as ecosystem engineers (Jones et al. 1994, 1997; Thomas et al. 2000). Caution is needed though as seagrasses do not always fit this label. In highly wave-exposed sites where seagrasses do not attenuate water flow as effectively as in unidirectional (tidal) flows (Koch and Gust 1999), sediment characteristics within and outside seagrass beds differed little to none (Hoskin 1983; Edgar and Shaw 1991; Koch 1999; van Keulen and Borowitzka 2001). Actually, in some cases, sediment in a vegetated area can be coarser than in the adjacent unvegetated area (Koch 1993; Fonseca and Koehl 2006; Koch et al. 2006).

4 How Waves Affect Seagrasses

Negative effects

Erosion/dislodgement

Landscape patterns observed in seagrass habitats are often associated with hydrodynamic disturbances (Fonseca et al. 1983; Fonseca and Bell 1998; Hemminga and Duarte 2000). As described in Koch et al. (2006), in areas disturbed by high wave energy, seagrass ecosystems can be: (1) non-existent (Dan et al. 1998); (2) depth restricted (when sufficient light is available, seagrasses colonize areas below the maximum wave penetration depth (Krause-Jensen et al. 2003; Middelboe et al. 2003); (3) dominated by more robust species (e.g., *Amphibolis griffithii* and *Posidonia coriacea*); or (4) patchier as the disturbance of high waves may hinder the lateral expansion of some seagrass beds (Kendrick et al. 2000; Frederiksen et al. 2004). In contrast, in sheltered waters, seagrass meadows tend to be more continuous and are colonized by relatively more fragile species (e.g., *Posidonia* spp) (Kirkman and Kuo 1990).

Recent developments (Koch, in preparation) suggest that seagrasses are resilient when exposed to waves (also see the following section). Their massive loss occurs when sediment becomes unstable due to erosion. Seagrasses can also be lost due to excessive sedimentation (Marbà et al. 1994; Walker et al. 1996; Bridgwood 2002; Paling et al. 2003, van Keulen and Borowitzka 2003; Frederiksen et al. 2004). Sand waves, a result of water flow, can lead to the deposition of tens of centimeters over periods of hours (Paling et al. 2003). The degree to which these large amounts of sediment negatively affect the seagrasses creating unvegetated patches depends on their tolerance to sedimentation, the amount of sediment deposited, and the period the plants remain buried. Some seagrasses (e.g., *Halodule wrightii*) are able to survive as long as the sediment is removed in a matter of weeks (Phillips 1980) while others (e.g., *Z. marina*) seem to have little or no tolerance to sedimentation regardless of the sediment type (Mills and Fonseca 2003).

Mechanical tissue damage

In wave swept environments, a long flexible shape (see Figure 3) can minimize the forces exerted on the roots of seagrasses. The long leaves tend to

move back and forth without fully extending, thereby minimizing the drag imposed on the roots (Koehl 1984).

The field of seagrass biomechanics is mostly unstudied. Kopp (1999) showed that strength of vegetative *Z. marina* shoots varies seasonally with the most vulnerable month (highest breakage) in September when the plants begin to senesce (i.e., when plants naturally lose their leaves due to shorter days and/or cooler weather). During this period, more than 50 percent of the leaves are unable to withstand 4.7 m/sec (current speed in seagrass beds is usually around 0.1 m/sec during calm conditions). Patterson et al. (2001) showed that reproductive shoots of *Z. marina* are as tough as macroalgae and that, among a population, a few reproductive shoots are extremely tough. These may persist even during hurricane forces ensuring the survival of at least some individuals (assuming that sediment erosion will not compromise the entire bed). Fonseca (1998) suggested that the force needed to damage live *Z. marina* may be achieved only infrequently under extreme storm conditions.

Turbidity

Seagrasses need relatively high light levels in order to thrive. Therefore, anything that increases water turbidity is detrimental to seagrasses. While sediments tend to be deposited in seagrass beds under calm conditions (see "Sediment stabilization" section in Chapter 3), some of these particles may be resuspended by waves during storm events. Seagrasses have acclimated to such relatively short (hours) pulsed high turbidity events. Turbidity events that last weeks or months (e.g., shoreline erosion, excessive river runoff, phytoplankton bloom) are the ones that lead to the loss of seagrasses (Moore et al. 1997). Additionally, wave-induced turbidity could potentially be detrimental to seagrasses when islands are lost or peninsulas breached due to erosion. This leads to a permanent increase in wave energy in areas that were relatively protected in the past. As a result, turbidity is expected to increase, especially in the beginning when fine particles deposited during more quiescent conditions are resuspended.

Positive effects

Flushing

Waves cause seagrass leaves to move back and forth. When leaves bend horizontally, they tend to isolate the sediment and water within the canopy

from the water column. Just a fraction of a second later, when the leaves are moved to a more vertical position by a passing wave, the canopy opens and the exchange between the water column and the seagrass canopy increases. The leaves then return to a more horizontal position starting the cycle over again. This constant leaf motion leads to extensive flushing of the seagrass bed possibly maximizing the flux of nutrients and carbon to the plant surface (Koch and Gust 1999).

Reduced self-shading and light-flecks

Seagrasses exposed to unidirectional flow (e.g., tidal currents) experience a high degree of self-shading as leaves lay on top of each other for extended periods of time. In contrast, wave-induced leaf flapping allows specks of light to penetrate the seagrass canopy at the frequency of flapping. As a result, higher productivity is expected in wave-dominated systems. Additionally, wave crests focus the light that reaches the water surface leading to short (fraction of a second) specks of high light levels referred to as light-flecks (Wing and Patterson 1993). The frequency of light-flecks resembles that of the passing waves (Koch et al. 2006). When seagrasses grow in shallow waters, they may benefit from these light-flecks. Although their effect on seagrass productivity was not yet tested, phytoplankton and macroalgae productivity is enhanced by light-flecks (Dromgoole 1988; Greene and Gerard 1990; Wing and Patterson 1993; Wing et al. 1993). It is assumed that seagrasses also benefit from light-flecks.

Pulses in the diffusive boundary layer

The diffusive boundary layer on seagrass leaves serves as a barrier to the free flux of nutrients and carbon to the plant surface. As a result, relatively stagnant conditions reduce the productivity of seagrasses (Koch 1994). Wave-induced oscillatory flows tend to disrupt the diffusive boundary layer for a fraction of a second. This process supplies pulses of molecules to the blade surface replenishing nutrients and carbon needed for plant growth (Nikora et al. 2002). Under wave-dominated conditions, these pulses occur on a regular basis enhancing productivity (Stevens and Hurd 1997).

Reduced epiphytic cover

Epiphytes are microalgae that grow on the surface of seagrasses blocking light and, when in excess, leading to the death of the plants. Epiphytic loading usually increases with nutrient availability. It has been speculated that waves and currents can lead to reduced epiphytic growth on seagrass leaves; little data are available to confirm this hypothesis. Pinckney and Micheli (1998) observed no difference in total epiphyte biomass in a wave-exposed and a sheltered seagrass habitat but noted that diatoms, coralline, and some filamentous algae dominate under wave-exposed conditions while blue green and other filamentous algae dominate under calm conditions.

Seagrass restoration in wave-dominated systems

Comparative studies of seagrass restoration across wave energy regimes are few. Individual studies show limited success in areas with high wave energy mainly due to mechanical removal of the plants and extensive sediment transport (van Katwijk and Hermus 2000; Paling et al. 2003; Campbell and Paling 2003). Sediment erosion and transport can be reduced by using shell (van Katwijk and Hermus 2000) or mats (when these stay in place; Campbell and Paling 2003) thereby increasing restoration success. Restoration success in areas of high wave exposure can also be increased when using larger size seagrass plugs (10 to 15 cm in diameter; van Keulen et al. 2003) although some seagrass habitats have such high wave energy (up to 50 cm s^{-1} orbital velocities near the sediment surface) that not even the largest seagrass sod units (0.5 x 0.5 x 0.35 m) remain in place (Paling et al. 2003). Increased turbidity in wave exposed areas could possibly also limit seagrass restoration, but this effect can potentially be mediated by oysters which filter suspended particles thereby increasing light availability (Newell and Koch 2004).

Except for a few studies, including the ones previously mentioned, comparative analyses of wave effects on restoration attempts remain largely anectodal or based on modeling exercises (Kelly et al. 2001). Fonseca et al. (1998) provide guidance on selection of sites and planting arrangement based on relative exposure of sites to waves, but this too is the result not of manipulative experiments but experience and correlations derived from study of natural seagrass landscapes (Bell et al. 1997). In general, if seagrass patches are expected to form, rather than continuous cover, then the wave climate exceeds the requirement for restoration. In this case, fre-

quent replanting efforts are likely to be necessary and may require as many as 50 percent of the original plant number.

5 Measuring Waves in Seagrass Systems

Introduction

Although seagrass habitats are influenced by currents and waves, studies focusing on seagrass hydrodynamics are few (Koch 2001). Those that address this topic focus mainly on currents. The study of waves in seagrass habitats is still in its infancy (Koch et al. 2006). As a result, methods used to quantify the wave climate and wave exposure in seagrass beds are few. Valuable suggestions can be drawn from the kelp literature as the study of waves in these systems is more advanced than in seagrass beds. Caution is needed though as waves in kelp beds are usually oceanic (long) in nature while those in seagrass beds are usually shorter. Therefore, waves need to be recorded at a higher frequency in seagrass habitats than in kelp beds.

Cartographic methods

In order for (most) waves to develop, wind needs to blow over the water. The longer the distance over which the wind can blow without encountering obstructions, i.e., the longer the fetch, the larger the waves can develop. As a result, the quantification of fetch is a simple method of approximating the wave exposure at a site. Cartographic methods are based on this principle.

Baardseth index of wave exposure

This index has not yet been used for seagrasses but is often applied in studies involving macroalgae (see Sjotun and Fredriksen 1995; Ruuskanen et al. 1999; and references therein). The Baardseth index can be determined by marking the study site on a nautical chart and drawing a circle around the study site. The circle is then subdivided into 40 sectors (9 deg each) and the number of sectors without any land obstructions such as peninsulas and island is counted. A high value indicates a high degree of wave exposure (i.e., few land obstructions to protect the site) while a value of 0 represents complete protection (i.e., site protected by land from all sides). The radius of the circle depends on the study site and the bottom topography. For example, Ruuskanen at al. (1999) used a radius of 7.5 km at a site surrounded by small islands. In contrast, Sjotun and Fredriksen (1995) used a series of circles/radiuses (0.5, 7 and 100 km) and calculated the Baardseth index for each radius (e_1, e_2, e_3) in an area surrounded by

islands but also affected by the local topography (a fjord). Total wave exposure (E) was then estimated using the following equation:

$$E = [e_1 + (10e_2) + (100e_3)].100 \quad (9)$$

Although simple to estimate, the Baardseth index does not take into account the dominant wind direction and intensity or the bottom bathymetry. This may lead to an overestimation of wave exposure especially in areas in which sills and sandbars occur. Sjotun and Fredriksen (1995) considered wind in the Baardseth index by assigning a relative wind force value (e) to each sector based on mean wind force and frequency over the last 5 years:

$$e = \frac{n_1 F_1}{100 S_1} + \frac{n_2 F_2}{100 S_2} + ... + \frac{n_n F_n}{100 S_n} \quad (10)$$

where S_n is the number of unobstructed sectors in a given direction, n_n is the number of observations of wind from a given direction and F_n is the average strength of wind from a given direction.

Relative wave exposure indices

Keddy (1982) took into account that a body of water affects its wave generation (e.g., although the fetch straight up a river may be long, the adjacent shorelines limit wave development) and considered effective fetch in the estimation of wave exposure in lakes colonized by freshwater plants. The effective fetch is estimated by measuring fetch along four lines radiating out from either side of a compass heading at increments of 11.25 deg. Keddy's relative wave exposure index (REI) also takes into account wind velocity, the dominant wind direction and exceedance winds:

$$REI = \sum_{i=1}^{8} (V_i \times P_i \times F_i) \quad (11)$$

where i = compass headings (1-8 (N, NE, E, etc.), in 45-deg increments), V = average monthly maximum wind speed in m/sec (or any other wind data of choice), P = frequency as a percentage of time wind occurred from the ith direction, and F = effective fetch (m). A detailed description of this index and how it relates to the distribution of submersed aquatic vegetation in lakes can be found in Keddy (1982). It appears that Keddy's wave

exposure index is capable of predicting submersed plant distribution in areas with steep slopes (e.g., some lakes) where waves are only affected by the bottom close to shore. In areas dominated by extensive shallow flats this index does not appear to hold because waves interact with the bottom (i.e., shallow waves) and, therefore, this leads to a disconnection between fetch (wave growth potential) and waves near the shore (combined growth and transformation).

The wave exposure index developed by Keddy has been applied to seagrass habitats by Fonseca et al. (2002). Although their relative wave exposure index (REI) was a good predictor of seagrass spatial distribution in some estuaries (Murphey and Fonseca 1995; Fonseca and Bell 1998), problems were encountered in other areas (i.e., Chiscano 2000). These were likely due to complex bottom bathymetry such as sills and sandbars. As a result, a further refinement of the wave exposure index, the relative wave exposure index now includes water depth and tidal fluctuations (Robbins et al. 2001):

$$REI = \sum_{i=1}^{8} \left[V_i \times P_i \times \left(idwF_i \times T_i \right) \right] \tag{12}$$

where an inverse distance weighting (IDW) function is used to weight effective fetch (F) by depth from the point of interest to the shoreline. Effective fetch is then further weighted by the period of tidal emersion (T) derived from a National Oceanic and Atmospheric Administration (NOAA) tidal prediction based on tide curves generated from harmonic analysis at gauge locations (readily available on NOAA's Web site).

A spatially explicit version of the relative wave exposure index, the Wave Exposure Model (WEMo) has been developed (Fonseca and Bell 1998; Kelly et al. 2001; Fonseca et al. 2002). WEMo calculates REI values at specified locations as a means of predicting the relative amount of wave exposure at each site. The model requires the user to input four variables: a bathymetric grid (ARC-based), a shoreline (shapefile), wind data (duration and speed from the eight major compass headings), and a file that defines georeferenced points or sites of interest. Model output includes a table that lists the REI value for each point, a shapefile of the points, and a contour plot of interpolated REI values. A recent calibration of WEMo results using wave height data collected in Chesapeake Bay suggest that

WEMo is a good predictor of wave exposure in shallow seagrass habitats especially when 25 and 50 percent exceedance winds are considered. At this writing, WEMo is being modified to repair a dimensionality problem, replace the IDW function with published wave decay functions as well as adding user-controlled selection of bottom friction values in order to embed the effect of seagrasses on waves following relationships described by Fonseca and Cahalan (1992). The model will be available for download from http://www.ccfhr.noaa.gov/ in late 2006.

Quantitative methods

Wave height and wave period are the most desirable parameters when studying waves in seagrass habitats. In order to understand sedimentary processes in vegetated areas it is also desirable to estimate the horizontal orbital velocity at the sediment surface. These parameters can be obtained through indirect calculations based on wind data (this section) or direct measurements using wave sensors (discussed later). Caution is necessary when estimating wave parameters based on wind speed, fetch and bathymetry as other parameters such as the presence of seagrasses, mussel beds, and oyster reefs, etc., can alter the wave climate. Therefore, these calculations should be used as estimates only and, whenever possible, should be calibrated against field wave data.

Estimating wave parameters based on wind and fetch data

To evaluate the success of *Zostera marina* transplants in the Dutch Wadden Sea (van Katwijk and Hermus 2000), significant wave height (average of the highest one-third waves, H_s) and period (T) were estimated using the Bretscheider method (SPM 1984):

$$\frac{gH_s}{u^2} = 0.283 \tan\left[0.530\left(\frac{gd}{u^2}\right)^{0.75}\right] \tanh\left[\frac{0.00565\frac{gF}{u^2}}{\tanh\left[0.530\left(\frac{gd}{u^2}\right)^{0.75}\right]}\right] \quad (13)$$

$$\frac{gT}{u} = 7.54 \tan\left[0.833\left(\frac{gd}{u^2}\right)^{0.375}\right] \tanh\left[\frac{0.0379\left(\frac{gF}{u^2}\right)^{0.333}}{\tanh\left[0.833\left(\frac{gd}{u^2}\right)^{0.375}\right]}\right] \quad (14)$$

where g is the acceleration of gravity; u is the wind velocity (m/s at 10 m above the water), d is the average depth along the fetch (m), and F is the fetch (m).

This method takes into account the bathymetry of the general area but only in the form of an average depth along the fetch. Therefore, in areas with sandbars or coral/oyster reefs this calculation overestimates wave parameters as the depth of the sandbar and/or reefs is likely to be only a small area of the fetch being considered.

Seagrass transplants can be compromised in areas of extensive sediment transport; therefore, an estimate of the horizontal orbital velocity (U) at the sediment surface may be useful when selecting a potential restoration site. Van Katwijk and Hermus (2000) estimated this parameter for a *Zostera marina* transplant site using the formula proposed by Visser (as described in Verhagen and van der Wegen 1998):

$$U = \frac{H_s}{2}\frac{2\pi}{T}\frac{1}{\sinh(kd)} \quad (15)$$

where $L = (gd)^{0.5}(1 - d/L_o)T$, g is the acceleration of gravity, d is the average depth along the fetch, and $L_o = 1.56\ T^2$. Once again, caution is advised as this calculation does not take into account local characteristics of the site that may alter the horizontal orbital velocity.

Measuring wave parameters in seagrass habitats

When measuring waves in seagrass habitats, the question to be addressed needs to be kept in mind. Is it necessary to determine the direction from which the waves are approaching the seagrass bed or will it suffice to determine wave height and period? Wave direction data may be relevant when sediment transport, pattern of seagrass bed expansion, seed dispersal or landscape characteristics are being considered. Wave direction is critical for estimating the magnitude and direction of wave-driven

longshore currents and the potential for seagrass beds to protect sediments and shorelines behind them. In contrast, nondirectional wave data may suffice when the questions posed address wave attenuation, local sediment resuspension, etc.

Quantifying nondirectional waves in seagrass systems

Visual estimations. As described in Morgan (2000), a simple and inexpensive way of quantifying waves is to make a visual estimation of wave height (vertical distance between troughs and crests) and period (time it takes two crests or troughs to pass a certain point) using a vertical reference pole. This method may be especially useful in areas with oceanic waves (long periods), but in areas with small and high-frequency waves such as those often found in estuaries, this method may be less reliable (Koch and Verduin 2001). To aid in the data gathering process, a video camera focused on the reference pole could be used and later analyzed at a slower speed. Even so, the data obtained using this method are limited.

Deployment of wave sensors. The use of wave gauges is recommended when quantifying wave parameters in seagrass beds where waves can often be relatively small in height and occur at relatively high frequencies. Wave sensors are capable of recording many times per second. These data are then analyzed to obtain the relevant wave parameters.

Selecting a wave gauge. There are a series of aspects that need to be considered when selecting a wave gauge:

a. Acoustic versus pressure sensors - Many wave measuring instruments currently on the market use acoustic techniques (Acoustic Doppler Velocimeter, acoustic profilers) while others use pressure transducers. The acoustic techniques are less desirable as seagrass leaves interfere with the acoustic beams (Koch and Verduin 2001). Even so, acoustic instruments can and have been used in seagrass beds (e.g., Gacia et al. 1999 deployed at 12-m depth; Verduin and Backhaus 2000 worked at 15- to 20-m depth) but the area where measurements are being taken needs to be cleared of seagrass leaves. This may lead to an alteration of the local hydrodynamic conditions. Additionally, seagrass debris and associated organisms such as fishes can still interfere with the acoustic beam. Filtering the data to eliminate these interferences is necessary when using acoustic instruments.

b. Water depth – Most wave gauges were developed for oceanic purposes. As a result, the pressure range of these gauges is often less suitable for shallow (< 3 m) seagrass habitats. For example, for work in shallow water, the oceanic instruments often offer pressure transducers in the 0 to 30 PSI range. In shallow seagrass habitats, a pressure transducer in the 0 to 5 PSI or 0 to 10 PSI would be more appropriate. Additionally, some instruments stop recording when exposed to air, therefore, the size of the instrument and the deployment depth should also be considered. The size of wave sensors has decreased in recent years as electronic components are becoming smaller and alternative methods for shallow-water deployment are now available. For example, in order to be suitable for shallow-water deployment, Acoustic Doppler Velocimeters and profilers can now be purchased with side looking probes such that the instrument can be laid on the sediment surface thereby occupying a smaller fraction of the water column.

c. Sampling rate – Oceanic waves are longer than estuarine and shallow-water waves. Therefore, a relatively low sampling rate (1 to 2 Hz) is suitable to describe oceanic waves. In contrast, higher sampling rates (2 to 5 Hz) are required to describe shallow-water waves. Therefore, caution is needed when selecting an instrument to record the short waves often observed in seagrass habitats. As illustrated in (Figure 8), the use of an instrument that uses a sampling interval, which is too large to resolve the relatively short waves in seagrass habitats, may lead to erroneous data. The sampling rate should be such that at least four samples are collected per cycle for the shortest wave present (Denman 1975). The highest frequency that can be resolved at a given sampling rate ν is referred to as the *Nyquist* frequency and is defined as:

$$f_{Nyquist} = \frac{1}{2}\nu \tag{16}$$

Note that this is two times higher than the highest resolvable wave frequency according to Denman (1975). For example, in the Chesapeake Bay, waves in seagrass habitats (1-m depth) frequently have periods of around 2 sec and frequencies of 0.5 Hz. Therefore, a sample rate of 2 Hz allows proper recording of these waves ($f_{Nyquist}$ = 1 Hz and f_{Denman} = 0.5 Hz). If significant wave energy exists in

frequencies higher than the *Nyquist* frequency, it will erroneously show up in lower frequencies in the analysis (aliasing).

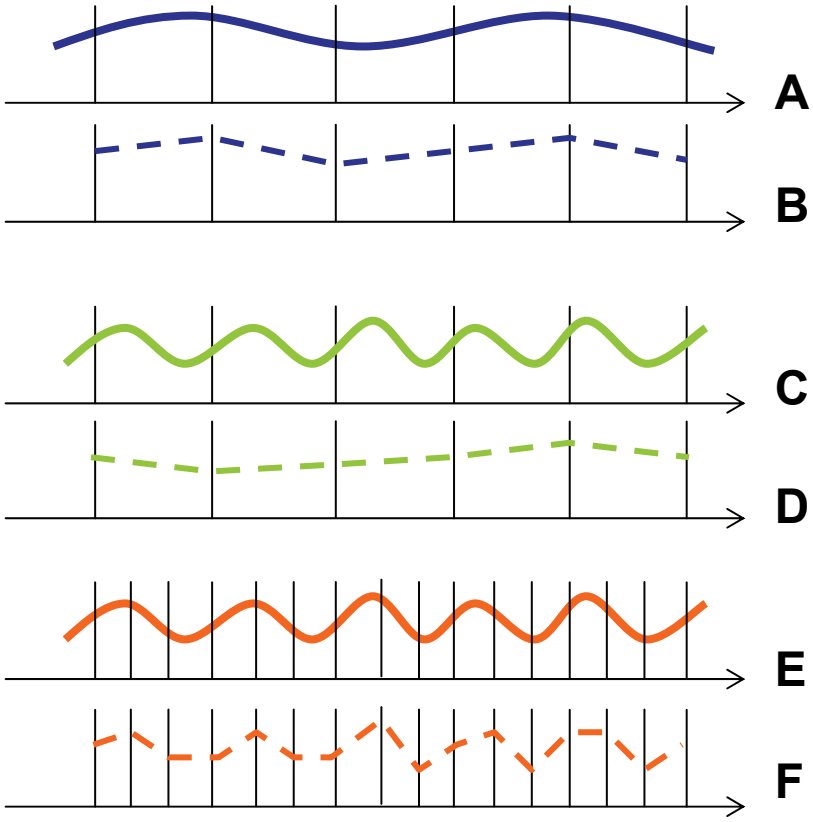

Figure 8. An example of how sampling rate affects the results of wave sampling protocols. The solid lines represent long/oceanic (A) and short/estuarine (C and E) waves. The x-axis represents time and each vertical line represents one sample. When the long wave (A) is sampled at relatively low rate (e.g., 1 or 2 Hz), its characteristics are relatively well represented by the data collected (B). When a short wave (C) is sampled at the same low frequency, the data collected are not a good representation (D) of the actual waves (C). In contrast, if the same short waves (E) are sampled at a higher rate, their characteristics are much better represented by the data collected (F).

d. Wave attenuation – Wave kinematics attenuate with depth (velocities and pressures are smaller at the bottom than near the surface). Thus, any near-bed measurements need to be designed so that the inherent noise in the measurements does not dominate the wave signal to be measured. For bottom-mounted pressure gauges, the linear transfer function used to convert the bottom measurement to the surface is $\cosh(2\pi d/L)^2$. For wavelengths (or periods) where this transfer function exceeds a value of approximately 100 to 1000, the measurement must be truncated and an important portion of the wave energy will be lost if the truncation period is not at least

half the peak wave period or shorter (Bishop and Donelan 1987; Smith 2002). For example, a bottom-mounted pressure gauge measurement must be in 2 m water depth or less to capture 3-sec waves, while 10-sec waves can be measured in water depths up to approximately 20 m. The presence of strong current can alter the wavelength and further limit the depth of measurement.

In summary, careful consideration is needed when selecting a wave sensor. It may be advisable to do a site visit and to identify the wave characteristics of the seagrass habitats to be studied prior to selecting an instrument. This could be done in collaboration with physical oceanographers or coastal engineers. Once general depth and wave characteristics for the study site are available, Table 1 can be used to guide the user in the instrument selection process.

Programming a wave sensor. Each wave sensor comes with its own software. The user programs the length of the bursts to be recorded as well as the sampling frequency. The sampling frequency needed to resolve the waves to be studied has been described. Therefore, this section will focus on the sampling design.

Waves are normally not recorded continuously over extensive periods of time (days or weeks) due to the volume of data generated. For example, a wave sensor recording at a 5-Hz rate will generate 4,500 data points in 15 min and 432,000 points in a day. Therefore, wave sensors are normally programmed to turn on for a determined period of time (or number of samples to be recorded) and then "sleep" until they are asked to record again. These time intervals during which the instrument is recording are referred to as bursts. The length of the bursts in seagrass research has varied from 5 to 13 min (Gacia et al. 1999; Verduin and Backhaus 2000; Koch 2002). A rule of thumb for wave data collection is to capture 100 to 200 dominant wave periods to get reliable statistics (e.g., 100 waves with a 3-sec period would be 5 min). Bursts are recorded at intervals predetermined by the user (Figure 9). The interval at which each burst is recorded depends on the amount of memory available as well as how often the wave conditions are expected to change. During storm events, a 30-min interval may be recommended while during calm conditions a 1- to 3-hr interval will suffice.

Table 1. Summary of wave sensors currently available on the market.

Sensor	Type	Directional	Minimum depth of deployment	Maximum sampling rate	Examples of Web links
Pressure transducer	Pressure (strain gauge)	No, unless 3 sensors are de-ployed	0.5 m	5 Hz	http://www.coastal-usa.com/
Electro-magnetic current meter w/ wave option	Pressure + electro-magnetic velocity	Yes or no (optional)	0.3 m	10 Hz	http://www.interoceansys-tems.com/s4options.htm
Vector velocimeter	Pressure + acoustic velocity	yes	0.1 m 0.5 m	64 Hz	http://www.nortek-as.com/hardware.php http://www.sontek.com/oceans.htm
Current meter and profiler	Pressure + acoustic velocity profile	yes	1 m	2 Hz	http://www.nortek-as.com/hardware.php http://www.sontek.com/oceans.htm
Acoustic wave and current profiler (AWAC)	Acoustic surface tracking + acoustic velocity profile	yes	2 m	4 Hz	http://www.nortek-as.com/hardware.php http://www.rdinstruments.com/waves.html http://www.sontek.com/oceans.htm

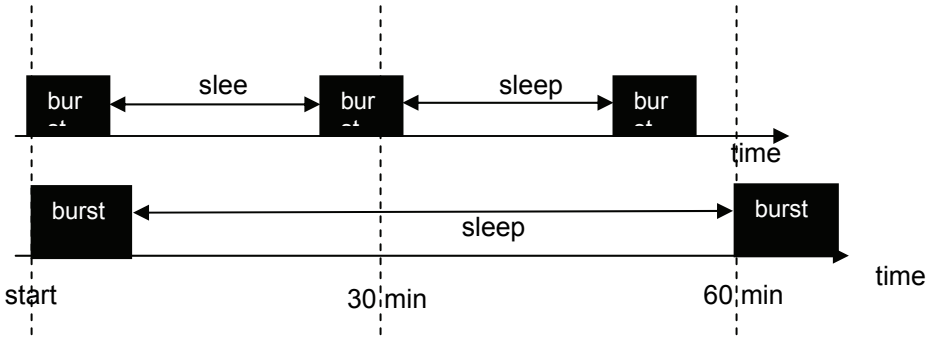

Figure 9. Schematic diagram of wave sensor sampling commonly used to record waves in seagrass habitats. The upper line represents a routine in which a burst (5 to 13 min) is recorded every 30 min while the lower line represents a routine where a burst is recorded every 60 min.

Deploying wave sensors in seagrass habitats. When quantifying waves in seagrass habitats, special attention needs to be given to:

a. Location of the instrument – the objective of the wave sensor deployment needs to be kept in mind. If the goal is to characterize the waves that reach a seagrass bed, the wave sensor should be deployed seaward of the seagrass bed where waves are not yet influenced by the vegetation. In contrast, if the goal is to characterize the waves in a seagrass bed, the sensor can be placed directly in the seagrass bed. In each case, the distance from the edge of the bed to the instrument should be recorded as well as the shoot density and canopy height. These data will be useful in the interpretation of data collected over several seasons and for different seagrass species. For deployment of more than one wave sensor, see following sections on quantifying direction waves and wave attenuation.

b. Stability of the instrument – it is essential that the sensor be securely attached to a solid structure. Even the slightest motion or vibration can cause false "waves" in the record. This can be accomplished by attaching the sensor to a tripod above the sediment surface or pipes or poles pounded or jetted into the sediment.

c. Interference with vegetation – if an acoustic instrument is used, the seagrasses need to be cleared from the sampling volume/path such that, even when the leaves bend over, they do not interfere with the acoustic signal. Therefore, the radius of the area cleared should be equal or larger than the maximum seagrass leaf length. This process is not necessary when using pressure transducers to quantify waves.

Data processing. When purchasing wave sensors, the manufacturer often provides software options for wave analysis. If that is not the case, Matlab (http://www.mathworks.com/) can be used to process wave data. The analysis required to obtain relevant wave parameters such as significant wave height and wave period is called Fast Fourier transformation. This analysis transforms a complex wave signal into a series of sinusoidal functions representing different wave frequencies (Figure 10). The amount of energy at each of these frequencies is then plotted in the form of wave spectra (Figure 11). The dominant (peak) wave frequency is then used to estimate the dominant wave period and the integral of the spectrum (wave energy) is used to calculate wave height. When waves propagate as swell, the peak is generally well defined and relatively narrow, while when the sea is choppy, the peak is less well defined and broader (Figure 11). Therefore, spectral width is also an interesting parameter to obtain. Addition-

ally, it is useful to plot the wave spectra instead of just analyzing the numerical parameters generated by the program. When two dominant wave frequencies occur, double peaks are observed in the spectra. Generally, software only analyzes the highest peak but the secondary peak may be biologically relevant. For example, while wind waves in the seagrass habitat may generate one peak in the spectra, the seagrass leaf flapping frequency may generate a second, smaller peak. The spectra can also provide a check on data quality, e.g., an increasing high-frequency tail on a spectrum could indicate sensor noise overwhelming the signal (cutoff too high) or unresolved higher frequency waves (cutoff too low).

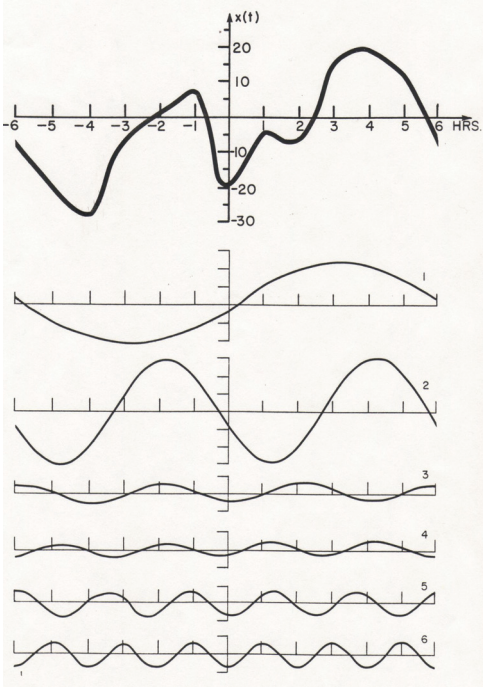

Figure 10. Visual representation of the wave breakdown process undertaken in the Fast Fourier analysis. The original complex signal (bold line on top) is decomposed into a series of sinusoidal functions representing different wave frequencies (thinner lines). The amount of energy in each wave/frequency is then plotted in the form of a wave spectrum (Figure 11).

Quantifying directional waves in seagrass systems

To measure directional waves requires a combination of at least three simultaneous measurements of pressure, velocity, sea-surface slope, sea-surface vertical velocity, sea-surface vertical acceleration, or sea-surface elevation. There are various combinations of these measurements that can provide the necessary information to calculate directional wave spectra; typical examples are pressure and two velocity components at a point location as with a 2 axis current meter equipped with a pressure sensor (PUV

meter), three (or more) simultaneous pressure measurements that are separated in space by precisely known geometry as with a pressure sensor array, or sea-surface slope, vertical velocity, and vertical acceleration as with a wave-rider buoy.

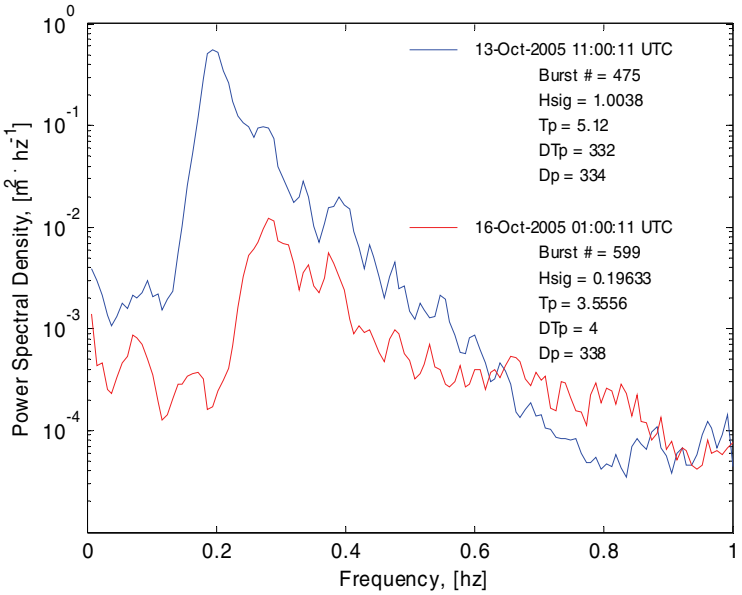

Figure 11. Nondirectional wave spectra for two wave bursts recorded on the eastern side of the Virginia portion of Chesapeake Bay between Nassawadox Creek and Hungars Creek. The data were collected with a 5-MHz Acoustic Doppler Velocimeter (ADV), equipped with a pressure gauge, and mounted to a bottom landing tripod deployed in 3-m water depth. Burst number 475 (blue line) shows a sharp peak at 0.2 Hz with a sharp decline in energy at higher frequencies, representing a narrower, well-defined wave train. Burst number 599 (red line) shows a flatter response with a broad peak and less fall-off of energy at higher frequencies, representing a more chaotic, choppy sea state.

Recently, Acoustic Doppler Current Profilers (ADCP) have become popular tools to measure directional waves. These instruments utilize spatially separated velocity measurements, acoustic beam surface tracking, and pressure data all from a single instrument.

Measuring directional waves in seagrass beds presents some challenges that limit the options for making these measurements. Many of the currently popular techniques for measuring waves and currents involve acoustic instruments, but they do not perform well in shallow seagrass beds due to interference of the seagrasses themselves with the acoustic beams of the instruments, and also due to the shallow-water depth, often less then 2 m in turbid waters. PUV gauges using electromagnetic velocity sensors are perhaps one alternative for measuring directional waves in

seagrass beds, but Howell (1998) described a technique using Short Base Line Arrays (SBLA) with three pressure sensors mounted in an equilateral triangle configuration that appears to be a better option. This technique offers many advantages such as reasonable cost, low maintenance, and well established analysis procedures. These SBLAs have sensor spacings (Howell used 1.8 m) that are significantly shorter than a wavelength, even when used in shallow water with high frequency waves (e.g., peak period=2 sec, depth = 1 m, wavelength = 6.3 m). This feature allows calculations of sea-surface slopes which offer additional analysis options. One requirement is that the pressure sensors used on these arrays be of high quality and have a resolution of 0.001 decibars and an absolute accuracy of 0.01 decibars.

Howell (1998) thoroughly describes the computations and equations necessary to calculate directional wave parameters from SBLA data and offers useful suggestions on how to reduce data storage requirements and prolong deployments. For noncommercial use there is a publicly available tool, "DIWASP, a directional wave spectra toolbox for MATLAB®" (see Figure 12 for an example of the output), that offers three of the most widely used contemporary analysis methods for directional waves. The DIWASP toolbox and User's Manual can be downloaded at: http://www.cwr.uwa.edu.au/~johnson/diwasp/diwasp.html.

Quantifying wave attenuation by seagrasses

Wave attenuation in kelp or seagrass beds is usually determined by measuring waves before they reach the vegetation and after they have passed through a certain distance of vegetated bottom (Figure 13). Therefore, when quantifying wave attenuation, at least two wave sensors are needed. If more sensors are available, a series of them can be deployed along a line perpendicular to the shore going through the seagrass bed and to an area offshore of the seagrass bed (Figure 13). This will allow wave attenuation to be quantified for different areas of the seagrass bed: edge, center, etc.

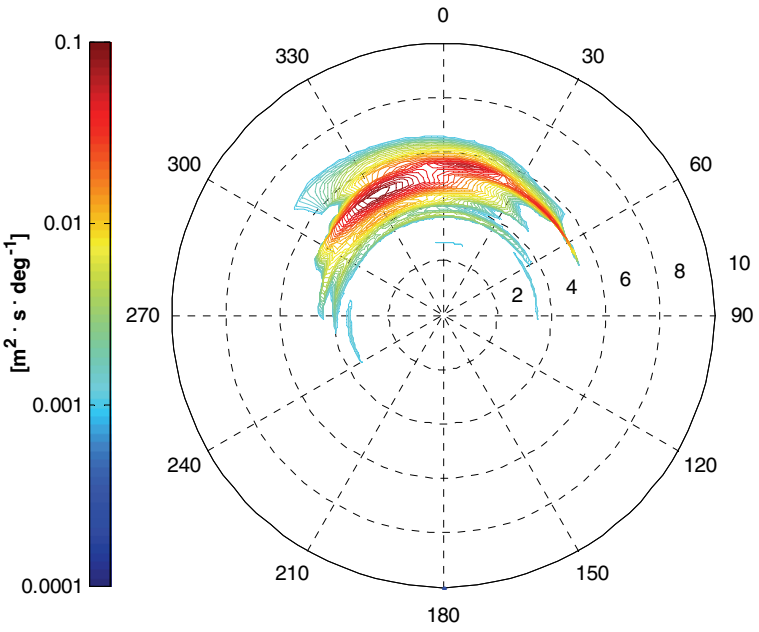

Figure 12. Polar plot of directional spectrum for burst number 475 (see Figure 11 for additional information). Directional spectrum was computed with "DIWASP, a directional wave spectra toolbox for MATLAB®", using the Iterative Maximum Likelihood Method (IMLM). Radial distances indicate wave period in seconds and color contours are power spectral density which is a measure of the energy content coming from a certain direction (in this case, mainly from the NE and N but also NW). For location and methods see legend of Figure 11.

Waves are not only attenuated by the vegetation but also over depth. As a result, it is recommended that the wave sensors be deployed at the same depth. This can be accomplished by installing poles or placing tripods at the sampling site and attaching the wave gauge at the appropriate height. If that is not possible, a depth correction will be required. Huber (2003) accounted for wave shoaling in a *Z. marina* bed by applying the following equation:

$$A_2 = A_1 \sqrt{\frac{c_{g_1}}{c_{g_2}}} \tag{17}$$

where A_1 and A_2 are the wave amplitudes ($A=H/2$) at the deep and shallow sites, respectively; c_{g1} and c_{g2} are the group velocities at the deep and shallow sites, respectively (Equation 8).

The shoreward edge of seagrass beds is usually defined by increasing depth. Therefore, the deployment of a wave sensor offshore of the seagrass

bed at the same depth of the sensor deployed in the seagrass bed may be difficult. An alternative may be to deploy one wave sensor in the seagrass bed and one in an adjacent unvegetated area which has the same depth and fetch (Figure 13).

In order to appropriately interpret the results, the distance from the wave sensor to the edge of the seagrass bed should be measured in different directions (all possible incident wave directions). If resources are available, it may also be useful to determine seagrass canopy height and shoot density in the area. This will allow for interpretation of wave attenuation as a function of these seagrass parameters.

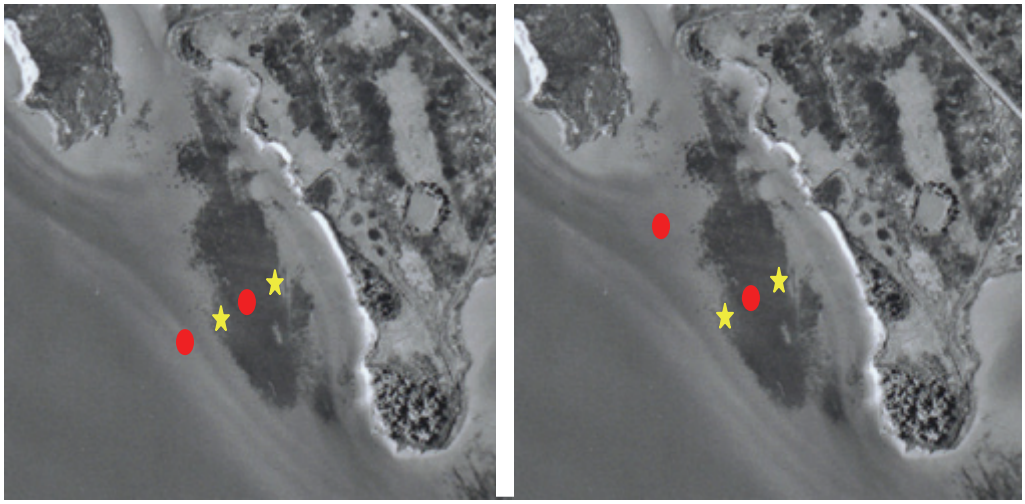

Figure 13. Alternative ways of deploying wave sensors when quantifying wave attenuation by seagrasses. The dark area adjacent to Bishop's Head Point, MD, shows a *Ruppia maritima* bed. The left panel gives an example of how wave sensors (red ovals and yellow stars) can be deployed along a shore-perpendicular transect. Ideally, all sensors will be at the same depth. The right panel gives an example of how wave sensors can be deployed at the same depth. Red ovals represent essential wave gauges while yellow stars represent suggested locations for additional sensors.

Wave sensors should be programmed to record waves concurrently. The data can then be plotted as wave height offshore versus wave height in the seagrass bed (Figure 14). The points usually falls below the 1:1 line indicating that there is wave attenuation. The slope of the regression line indicates the degree of attenuation of waves by the seagrass bed (Figure 14). In addition to plotting the data, it should also be processed by determining wave attenuation (AT) as the percentage of the original (offshore) wave height (H_o) still observed in the seagrass bed (H_s):

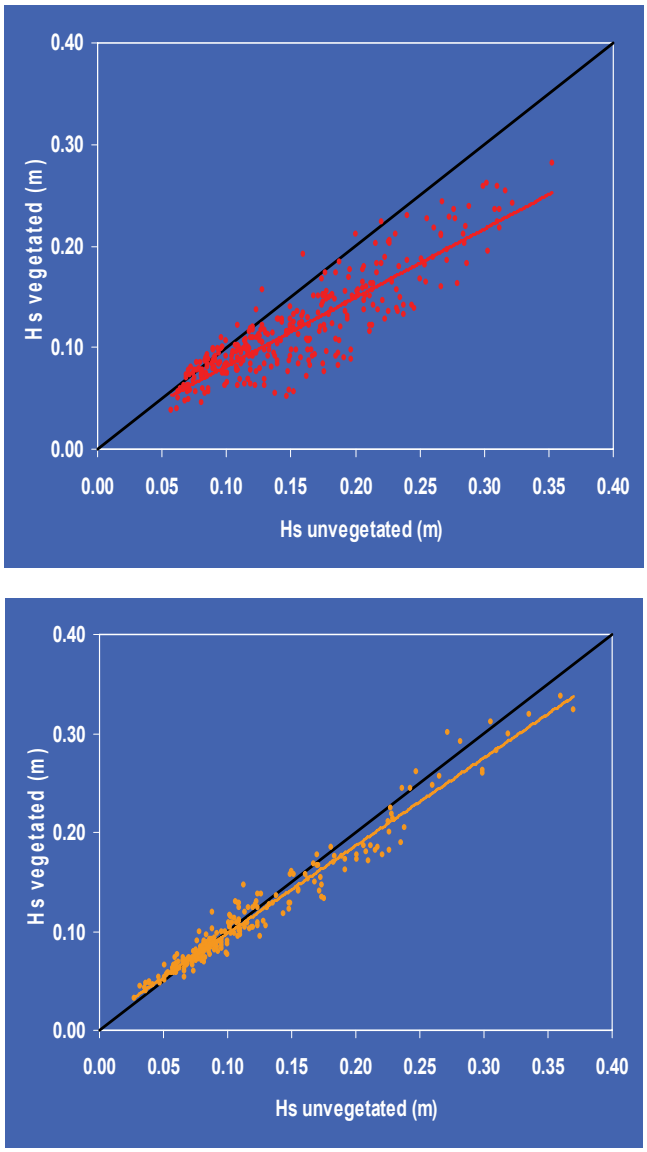

Figure 14. Wave attenuation in a seagrass (*Ruppia maritima*) bed off Bishop's Head, MD, in June (top) and October (bottom). In June, shoot density was 1,270 shoots m^{-2} and plants were reproductive (occupied the entire water column) while in October the shoot density was 1,968 shoots m^{-2} and plants were not reproductive occupying only a fraction of the water column. The black line represents the 1:1 slope, i.e., no wave attenuation. Note the higher wave attenuation in June than in October.

$$AT = \frac{H_s}{H_o}\sqrt{\frac{c_g}{c_{g_o}}} * 100 \tag{18}$$

The ratio of the group velocities accounts for shoaling due to differences in depth at the observation points (if depths are significantly different, changes in wave height due to refraction should also be considered). The results are usually expressed as a percentage of attenuation over a distance (e.g., percent/m or percent/100 m). Wave attenuation should be determined for each burst and then plotted as a time series of wave attenuation over time (Figure 15).

The principles described also apply to the quantification of waves in wave tanks. Caution is required in the wave generation process though. The waves generated in the lab should be relevant to those observed in seagrass beds. For example, if a wave generator is only able to generate 1-sec waves while local seagrasses are usually exposed to 3- or 4-sec waves, the attenuation obtained in the lab may not be relevant to the field populations.

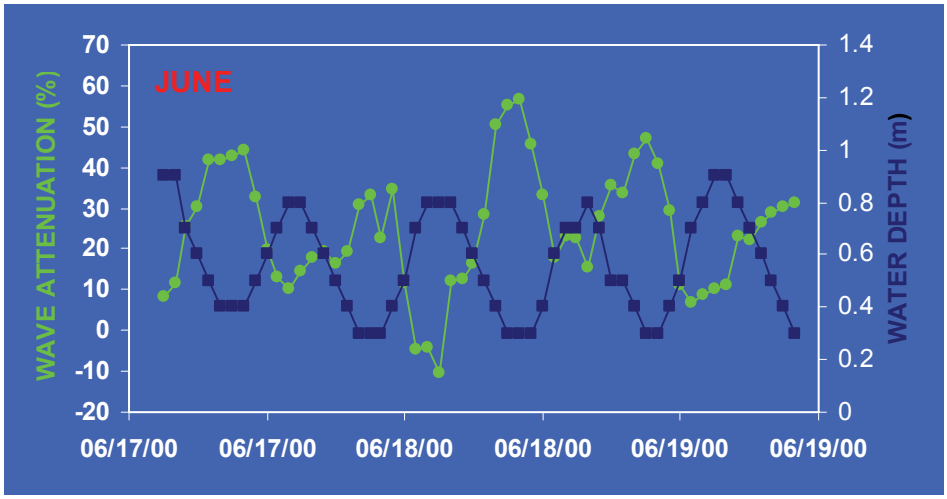

Figure 15. Wave attenuation in a seagrass (*Ruppia maritima*) bed off Bishop's Head, MD, in June when plants were reproductive and occupied the entire water column. Note that wave attenuation is a function of water depth: at high tide wave attenuation is low and at low tide wave attenuation is high.

6 Modeling Waves, Flow, and Sediment Transport in Seagrass Systems

Existing models

There have been relatively few modeling studies of interactions between waves, flow, and sediments in seagrass beds. Teeter et al. (2001) provide a comprehensive review of the physical, biological, and sedimentological complexities involved in any such effort and present relevant equations as a point of departure, but they do not present a complete model. They state that the primary limitations on developing a complete wave-flow-seagrass-sediment model are computational power and information on the frictional damping and bottom sheltering effects of seagrass beds. In the face of continuing improvements in computing power, frictional damping and bottom sheltering in seagrass beds remain as the key issues.

In fact, wave/flow damping by aquatic vegetation has been the focus of several previous modeling studies. These studies have focused on development of expressions and parameterizations for 1- or 2-D frictional drag, in terms of a vegetation Reynolds number and/or vegetation density. The drag force of the vegetation on the flow is usually expressed as:

$$F = \frac{1}{2}\rho \overline{f} a U^2 \tag{19}$$

where F is force per volume, a is projected area per volume, $\overline{f}$ is the bulk drag coefficient, and U is the maximum wave-induced velocity or flow speed. The projected area a is expressed as nd in Nepf (1999)'s cylinder model for steady currents, where n is the number of shoots per unit bottom area and d is a typical shoot diameter. This definition of a is similar to $N \cdot b_v$ in the wave damping models by Kobayashi et al. (1993); Mendez et al (1999); Mendez and Losada (2004);and Ota et al. (2004) where $N = n$ = the number of shoots per unit bottom area and b_v is defined as the plant area per unit height. Selected summaries of previous studies are presented in the following paragraphs.

Kobayashi et al. (1993) presented an analytical solution of wave height decay through vegetation based on linear wave theory, a Reynolds number dependent drag parameterization, and constant depth. They compared

their model to flume studies on artificial kelp stands (N = 1100 and 1490/m², b_v = 52 mm). The flume studies consisted of 60 runs with varying water depths (0.45-0.52 m), wave periods (0.714-2 sec), and wave heights (0.036-0.1934 m). They used the bulk drag coefficient ($\overline{f}$) to calibrate the model for 60 runs and then correlated $\overline{f}$ with Reynolds number ($R = Ud/\nu$, where ν is the kinematic viscosity of the water). They found that $\overline{f}$ decreases with increasing Reynolds number, and the relationship can be approximated by:

$$\overline{f} = 0.08 + \left(\frac{2200}{R}\right)^{2.4} \tag{20}$$

Equation 20 is plotted in Figure 16a.

Mendez et al. (1999) and Mendez and Losada (2004) expanded Kobayashi's solution by including swaying motion of the seagrass, wave breaking, and variable depth, and parameterized their model based on careful flume experiments. They allowed for swaying motion of the seagrass by changing the characteristic velocity in Equation 19 to the relative velocity between plant and water. They reported another empirical relationship between bulk drag and Reynolds number:

$$\overline{f} = 0.4 + \left(\frac{4600}{R}\right)^{2.9} \tag{21}$$

Equation 21 is also plotted in Figure 16a. Given the same Reynolds number, the bulk drag coefficient in Mendez et al. (1999) is higher than that in Kobayashi et al. (1993) because a lower velocity relative to the plant when accounting for plant motion requires a higher drag coefficient to maintain the same amount of wave energy attenuation. Their model fit to the data has a better correlation coefficient than Kobayashi et al.'s model, which suggests that swaying motion of plant might need to be considered for optimal drag estimation.

Nepf (1999) used a different approach to explore the drag of vegetation on steady currents. She ignored the flexibility of the vegetation, mimicking the seagrass stalks using arrays of cylinders (width d = 6.4 mm). Based on observations for pairs of cylinders by Bokaian and Geoola (1984), she assumed that the bulk drag coefficient is a function of vegetation density as represented by the fractional volume occupied (ad). Numerical simula-

tions were then performed for both random and staggered arrays of cylinders with different element spacings (different values of *ad*). She showed that the bulk drag coefficient is relatively constant for *ad* up to 0.01 and declines steadily beyond this density (Figure 6 in Nepf 1999). An approximate fit to her data (Equation 25) is plotted in Figure 16b. In the density-independent range (0.001<*ad*<0.01), the spacing between cylinders is too large for the wake behind an upstream cylinder to influence the drag of a downstream one. In the steady-decline range (0.01<*ad*<0.1) the drag coefficient decreases due to turbulent wake interference that delays the point of separation on a downstream cylinder and subsequently leads to a lower drag (Kundu and Cohen 2002). It should be noted that in this model $\overline{f}$ was argued to be a weak function of Reynolds number.

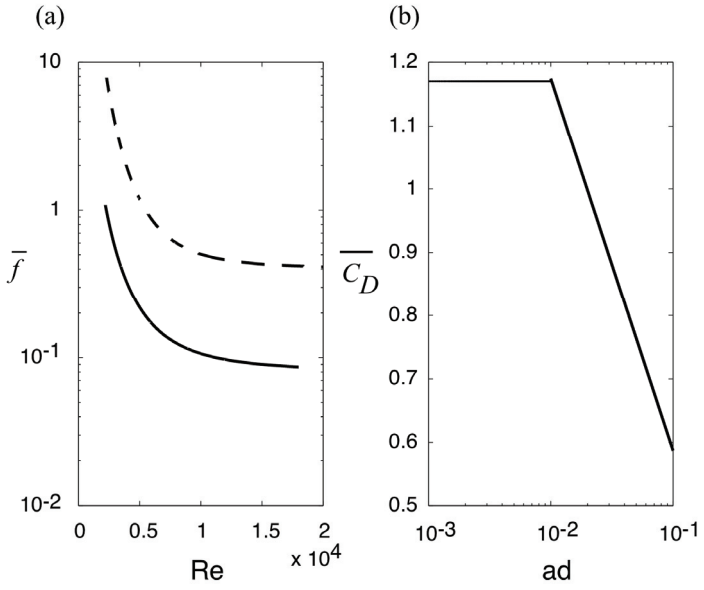

Figure 16. (a) Relationship between the bulk drag coefficient ($\overline{f}$) for pure wave motions and Reynolds number (Re). The solid line (Equation 20) is the relationship reported in Kobayashi et al. (1993), whereas the dashed line (Equation 21) is from Mendez et al. (1999). (b) Approximation (Equation 25) of relationship between the bulk drag coefficient ($\overline{C_D}$) for steady current and the fractional volume occupied by vegetation (*ad*) reported in Nepf (1999).

There are two main differences between drag models following Kobayashi et al. (1993) and the model of Nepf (1999). First, Kobayashi-type models are for oscillatory flow (waves) while Nepf's model is for steady currents. Therefore, the Reynolds numbers are different because the characteristic velocities (*U*) are wave orbital velocity and uniform current speed, respectively. Second, in Kobayashi-type models the bulk drag is a function of

Reynolds number that reflects the nature of the flow around a single shoot of vegetation. In contrast, the bulk drag in Nepf's model is a function of vegetation density that reflects a property of the whole bed. The flume experiments presented in Kobayashi et al. (1993) and Mendez et al. (1999) have an equivalent $ad \sim 3$. This value is above the range of ad (0.001~0.1) reported by Nepf (1999); note that the Nepf values are more representative of natural seagrass beds. The high vegetation density in the Kobayashi et al. (1993) and Mendez et al. (1999) studies implies a strong vegetation density dependence according to the results of Nepf (1999), although oscillatory motion may have limited the growth of turbulent wakes. On the other hand, the fact that the Nepf (1999) study was for steady currents limits its direct applicability to wave-seagrass interactions.

All of these studies were vertically two-dimensional (2-D), measuring or modeling a vertical slice through a seagrass bed in the direction of wave propagation or flow, with flow prevented from diverging around the bed. Thus, while they were all instructive and valuable, they could not consider spatially varying seagrass bed geometry (e.g., less than complete seagrass coverage), spatially varying shorelines and bathymetries, or combinations of waves and currents. In addition, although there have been several observational studies that indicate enhanced sediment deposition in seagrass beds (Lopez and Garcia 1998; Gacia et al. 1999; Gacia and Duarte 2001; Koch et al. 2006), there have been almost no modeling studies of sediment transport in seagrass beds.

The model described by Teeter et al. (2001), as implemented at least partially in Teeter (2001), is an exception. It is quite comprehensive, including wind forcing, wave forcing, seagrass-enhanced drag, and sediment transport, but it depends extensively on empirical parameterizations based on local observations. For example, Teeter (2001) implemented this model for Laguna Madre, TX, representing vegetation drag by a fixed roughness ($k_n \sim 0.2$ m) which was tuned to give reasonable agreement with field observations, but is not applicable to seagrass beds in other locations with other combinations of waves and currents.

Given these shortcomings, a new approach was developed for modeling interactions between waves, currents, and sediment transport in seagrass systems. The new model reduces the empiricism of the Teeter et al. approach by estimating wave and current drag that depends on seagrass density and height, based on Nepf (1999). It also considers three-

dimensional (3-D) spatial variability in bed geometry and bathymetry, allows for both wave and current influences, considers the nearshore currents generated by wave breaking, calculates total bottom shear stress based on vector addition of wave and current stresses, and estimates fine sediment resuspension, deposition, and transport in and near grass beds. In the remainder of this section, the model development is described with an emphasis on drag estimation, validate it against flume studies of flow reduction by Gambi et al. (1990) and against field observations of wave damping (Koch, unpublished), and present several model scenarios exploring the effects of seagrass bed geometries on wave attenuation, tidal current modification, and sediment trapping.

Model development and validation

Numerical modeling of waves and currents

A quasi-3D, curvilinear version of the nearshore circulation model SHORECIRC with wave driver REF/DIF (Kirby and Dalrymple 1994; Shi et al. 2003) has been adapted. This modeling system, supported by the U.S. Nearshore National Ocean Partnership Program (NOPP), aims to predict current, wave, and wave-driven current transformations in the nearshore ocean. SHORECIRC numerically solves the depth-integrated 2-D horizontal equations and incorporates a semianalytical solution for the vertical current profile (Svendsen et al. 2000). REF/DIF accounts for shoaling, refraction, energy dissipation, and diffraction as waves propagate over variable bathymetry and determines short-wave forcing to drive currents in SHORECIRC. Enhancements to the system include estimating seagrass effects on drag and turbulence, calculating the vector sum of wave and current bottom stresses, and adding a fine sediment transport module.

For the model presented here, the vegetation form drag expression of Nepf (1999), which was developed based on laboratory experiments with steady flows through rigid grass mimics, was adopted and modified. The primary reason for using this expression is that it explicitly accounts for the effects of seagrass shoot density over a realistic range of densities. The dominant seagrass species in the field studies to which model predictions was compared was *Ruppia maritima* (leaf width ~ 1.5 mm), with a fractional volume (*ad*) that fluctuated seasonally between about 0.0014 and 0.003. This range of *ad* is within the density-independent regime of Nepf (1999), but it is three orders of magnitude smaller than the values reported in Kobayashi et al. (1993) and Mendez et al. (1999) for their laboratory studies of sea-

grass wave drag. Steady flow drag data in comparable seagrass densities were preferable to wave drag data from a much higher seagrass density, especially since the same basic drag formulation for both steady flow and wave forcing in the model was used.

Bottom shear stress for steady currents is written using a standard quadratic law:

$$\tau_c = \rho C_d U^2 \tag{22}$$

where ρ is flow density, U is depth-averaged flow velocity, and C_d is the drag coefficient. Assuming that seagrass blades may be modeled as rigid cylinders, Nepf (1999) partitioned drag into skin friction due to contact between flow and sediment grains and form drag by the seagrass blades. She expressed the drag coefficient as:

$$C_d = (1 - ad)C_B + \frac{1}{2}\overline{C_D} ad \left(\frac{h}{d}\right) \tag{23}$$

where a is the projected plant area per unit volume, d is shoot diameter, h is water depth, ad represents the fractional volume occupied by seagrasses, C_B is a skin friction drag coefficient (set equal to 0.001 here), and $\overline{C_D}$ is the bulk drag coefficient for seagrass, which Nepf (1999) determined from experiments. The first term on the right-hand side of Equation 23 represents skin friction, whereas the second term represents form drag. The calculation of a was modified to allow seagrasses to only occupy part of the water column, so $a = nld/h$, where n is the number of seagrass shoots per unit area and l is the shoot height. Substituting into Equation 23, the drag coefficient for current becomes:

$$C_d = \left(1 - \frac{nld^2}{h}\right)C_B + \frac{1}{2}\overline{C_D} nld \tag{24}$$

Thus, it is a function of shoot height, shoot density, shoot diameter, and water depth. In Nepf (1999)'s model, the bulk drag coefficient is a function of fractional volume (ad). We approximate the curve in Figure 16b of Nepf (1999) as:

$$\overline{C_D} \approx \begin{cases} 1.17, & 10^{-3} < ad < 10^{-2} \\ -0.255 \ln(ad), & 10^{-2} < ad < 10^{-1} \end{cases} \tag{25}$$

In Nepf's experiments the velocity was measured at 7.5 cm above the bottom, whereas the reference height in SHORECIRC was set at 1 m. Hence, the drag coefficient for 7.5 cm height needs to be converted to that for 1 m. Assuming that the near-bottom velocity profile is logarithmic, we calculate the bottom roughness coefficient z_o using the well-known relationship between the drag coefficient and the bottom roughness parameter in a rough turbulent boundary layer (Equation 26). C_d is obtained from Equation 24 and reference height z equal to 7.5 cm; k is the von Karman constant, equal to 0.4.

$$C_d = \left[\frac{k}{\ln\left(\frac{z}{z_0} \right)} \right]^2 \tag{26}$$

Finally, using this z_0 and a new reference height of 1 m, the drag coefficient for SHORECIRC is obtained.

Field observations were used to determine the seagrass bulk drag for waves in REF/DIF. Bottom shear stress due to pure wave action (τ_w) is expressed in terms of the wave friction factor (f):

$$\tau_w = \frac{1}{2} \rho f u_b^{\,2} \tag{27}$$

where

$$f = \left(1 - \frac{nld^2}{h} \right) f_B + \frac{1}{2} \overline{f} hld \tag{28}$$

where u_b is wave orbital velocity near bottom, f_B is the wave skin friction factor, and $\overline{f}$ is a bulk drag representing the effects of seagrasses on waves. f_B was calculated using a bottom roughness equivalent to the value of C_B = 0.001 used in SHORECIRC, following procedures in U.S. Army Corps of Engineers (2002), while $\overline{f}$ was determined using field observations and assuming the functional form of Equation 25 with an adjustable multiplicative coefficient.

Once the drag coefficient and wave friction factor are estimated through Equations 24 and 28, current and wave fields are calculated by SHORECIRC and REF/DIF. With this updated current and wave field (wave height and period) and with known bottom sediment grain size, skin friction shear stress due to pure current (τ_{cs}) and wave motions (τ_{ws}) can be obtained using the techniques in U.S. Army Corps of Engineers (2002). Then we apply vector summation of the two skin friction components to calculate maximum skin friction shear stress (τ_{ms}) as follows:

$$\tau_{ms} = \sqrt{(\tau_{ws} + \tau_{cs}\left|\cos\phi_{wc}\right|)^2 + (\tau_{cs}\sin\phi_{wc})^2} \tag{29}$$

where ϕ_{wc} is the angle between current and wave propagation and can be calculated from SHORECIRC and REF/DIF. Because we are interested in the maximum potential for sediment movement, the absolute value of $\cos\phi_{wc}$ is used in Equation 29 to guarantee maximum vector summation regardless of the direction of wave orbital motion. This vector summation ignores enhanced turbulence due to nonlinear wave-current interactions in the bottom boundary layer (Grant and Madsen 1979). However, given the high uncertainty of seagrass drag estimation and turbulence structure in seagrass beds, Equation 29 is a reasonable first order approximation for combined wave-current bottom stress.

Sediment transport modeling

A suspended sediment transport module has been developed and incorporated based on North et al. (2004). The module accounts for erosion and deposition with a simple parameterization of consolidation for single-grain-size cohesive sediments. We solve for changes in bottom sediment per unit area (B in kg/m^2) over time t at each grid point using:

$$\frac{dB}{dt} = D - E - \gamma B \tag{30}$$

where D and E are the deposition and erosion rate (kg/m/sec), respectively, and γ is a first-order consolidation rate (sec^{-1}; set equal to zero here). The formulation states that the amount of erodible sediment per unit area increases by deposition but decreases by erosion and consolidation. The deposition rate is calculated as:

$$D = W_s C \tag{31}$$

where the settling velocity (W_s) is equal to 0.03 cm/sec (a typical value for fine suspended sediment in Chesapeake Bay, Sanford et al. 2001) and C is depth-averaged suspended sediment concentration (kg/m3). The erosion rate may be expressed as:

$$E = M(\frac{\tau_{ms}}{\tau_c} - 1)H(\tau_{ms} - \tau_c)H(B + 2\frac{dB}{dt}) \quad (32)$$

where τ_c is critical shear stress for erosion (e.g., approximately 0.15 Pa for fine sand), M is an empirical constant (5x10^{-5} kg/m/sec here), and H is the Heaviside step function (H=1 when its argument is > 0 and H=0 when its argument is ≤ 0). The first step function in Equation 28 represents the initiation of sediment motion when the maximum bottom shear stress exceeds the critical value, while the second step function is to prevent over-erosion and negative values of B.

Given the erosion and deposition rates in each model cell, a third-order accurate numerical scheme QUICKEST (Leonard 1979) is used to solve the depth-averaged transport equation for suspended sediments (Clarke and Elliot 1998):

$$\frac{\partial(HC)}{\partial t} + \frac{\partial(HUC)}{\partial x} + \frac{\partial(HVC)}{\partial y} = \frac{\partial}{\partial x}(HK_x\frac{\partial C}{\partial x}) + \frac{\partial}{\partial y}(HK_y\frac{\partial C}{\partial y}) + E - D \quad (33)$$

where H is water depth, U and V are depth-averaged velocity components, and K_x and K_y are diffusion coefficients. The QUICKEST scheme has been shown to avoid overshoot problems near strong gradients in concentration. This feature is particularly important because the presence of seagrass could lead to abrupt changes in bottom shear stress, which may in turn cause strong gradients in suspended sediment concentrations.

Model validation

First, the model to test the effects of seagrasses under current-only conditions (SHORECIRC only) was set up. Because we are particularly interested in modeling the effects of seagrass beds that cover only part of the model domain, such that water may flow around the bed rather than being forced through it or over it, the data of Gambi et al. (1990) was used for comparison. Gambi et al. studied flow speed reduction by *Zostera marina L.* (eelgrass) in a seawater flume, with the seagrass bed occupying only 20 percent of the width of the flume. SHORECIRC was configured to

mimic the relative dimensions of their flume experiments. The actual model domain was considerably larger because of computational constraints, but the ratios of the domain length, domain width, and the size of the eelgrass bed were scaled exactly. Flow was driven using an upstream flux boundary condition, with no flow through the domain sidewalls, to generate the same free-stream velocities as Gambi et al. The eelgrass parameters they reported were used to calculate the drag coefficient for SHORECIRC based on Equations 24 and 25. The volume flux reduction was computed within the eelgrass bed from just upstream of the bed to the end of bed, the same relative locations as in their flume measurements. The volume flux reduction is defined as:

$$(1 - \int Udz / \int U_{control} dz) \times 100 \tag{34}$$

where $U_{control}$ is the upstream velocity. Combinations of two shoot densities (600 and 1,200 shoots/m^2) and two free-stream velocities (10 and 20 cm/sec) were chosen. Comparisons are shown in Figure 17.

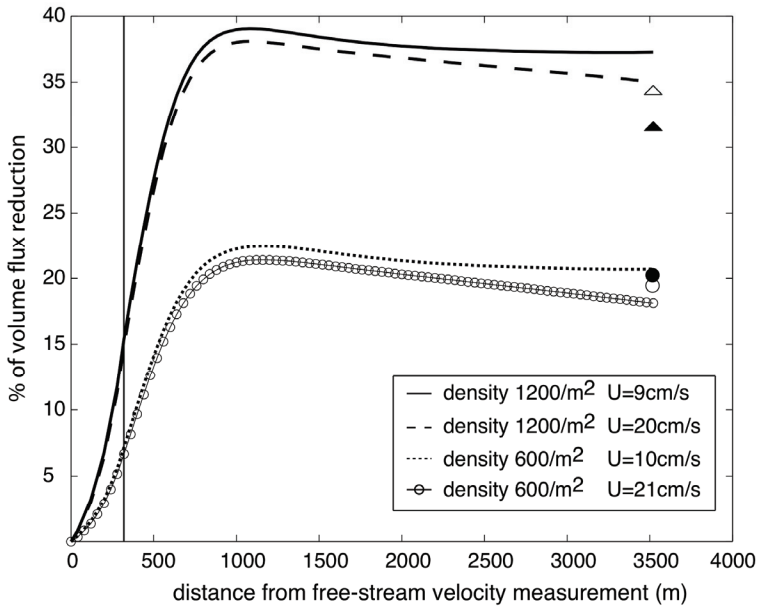

Figure 17. Comparison of flow speed reduction by a seagrass bed between model predictions (4 curves) and flume data reported by Gambi et al. (1990) (4 discrete points). The model is set up using the same relative dimension as Gambi et al.'s flume, and the same seagrass parameters such as shoot density, shoot height, and leaf width are applied. The percent of volume flux reduction is used as an indicator of flow speed reduction and is plotted against the distance downstream from the free-stream velocity measurements. The leading edge of the seagrass bed is indicated by the vertical line at 320 m. The open and solid triangles represent shoot densities of 1,200/m^2 with 20 and 10 cm/sec free-stream velocities, respectively, whereas the open and solid circles are 600/m^2 with 20 and 10 cm/sec.

The model-predicted values for the four different combinations agree reasonably well with Gambi et al.'s results, without any parameter tuning. As expected, the eelgrass bed with higher shoot density results in higher volume flux reductions. The model-predicted volume flux reduction increases rapidly behind the leading edge of eelgrass bed and levels off approximately halfway into the bed.

Next, the model was set up to test the effects of seagrass on wave attenuation (RED/DIF only). As mentioned already, the formulation (Equation 28) for estimating the wave friction factor has a similar functional form as that for steady currents. However, equivalent data to that of Nepf (1999) on the relationship between seagrass density and wave form drag $\overline{f}$ is not available. Therefore, field observations were used to determine the magnitude of the wave form drag. The field observations were carried out in Duck Point Cove, near Bishop's Head Point, MD, in mesohaline Chesapeake Bay (Newell and Koch 2004). Time series of wave height and seagrass parameters were measured in different months at two adjacent sites parallel to the shoreline, one vegetated with *R. maritima* and the other unvegetated. The size of *R. maritima* bed was about 600 m in the alongshore direction and 200 m in the cross-shore direction, and a pressure sensor was located at the center in average water depth of 1 m. Assuming the same incident wave climates at the two sites, wave height measurements can be plotted at the unvegetated site against the vegetated site to evaluate wave attenuation by the *R. maritima* bed. Assuming that $\overline{f}$ is a function of fractional volume (*ad*) and has similar functional form to that for steady current (Equation 25), the height of the $\overline{f}$ curve was changed to obtain the observed wave attenuations in October. The calibrated $\overline{f}$ is written as:

$$\overline{f} \approx \begin{matrix} 0.253, & 10^{-3} < ad < 10^{-2} \\ -0.055\ln(ad), & 10^{-2} < ad < 10^{-1} \end{matrix} \tag{35}$$

Applying observed seagrass parameters for May and June, the corresponding wave friction factors were calculated and the model-predicted wave height with observations were compared. Figures 18 (a), (b), and (c) show the comparisons in May, June, and October, respectively.

Wave attenuation by the seagrass bed peaks in June when the shoot height occupied the whole water column as a result of the development of reproductive shoots. The slope of the linear fit between the unvegetated and

vegetated wave heights in June was 0.68 (a slope of 1 means no wave attenuation). The model qualitatively captures this trend (June > May and Oct) although the model tends to slightly underestimate wave attenuation in June.

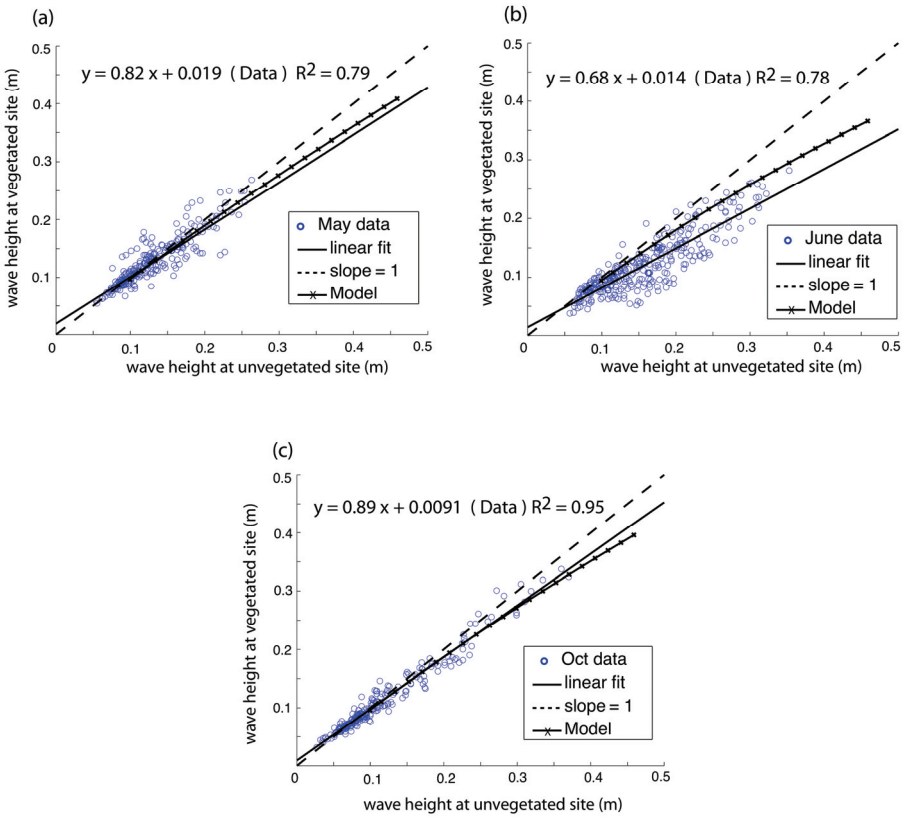

Figure 18. Comparison between model-predicted wave attenuation by a seagrass bed and field observations. Each panel shows field data (open circle), linear fit of field data (solid line and regression function), 1:1 slope (dashed line), and model prediction (-x-) for a month. The shoot density of *Ruppia maritima* bed is about 1536, 1270, and 1968/m² for May (a), June (b), and October (c), respectively, and the corresponding canopy height is 0.4, 1.0, and 0.4 m. The model is calibrated by use of October data (see text). The 1:1 line represents no wave attenuation. From the linear regression of field data, wave attenuation is higher in June than in May and October due to the presence of long reproductive shoots.

This approach has the advantage that a wider range of vegetation density is covered with one empirical parameter ($\overline{f}$). This is particularly useful for simulating seasonally or geographically varying seagrass populations. The underestimation of wave attenuation in June may be due to a different response to oscillatory forcing, the flexibility of natural seagrass blades, or a Reynolds number dependence not accounted for. However, for the present purpose the fact that a qualitative reproduction of changing wave drag was achieved due to seasonal changes in seagrass morphology is consid-

ered to be sufficient. Further study is needed to understand seagrass bulk drag accounting for all of these effects as well as a wide range of realistic vegetation densities.

Model scenarios

The model domain is set at 720 m in the shore-normal direction and 5,400 m in the shore-parallel direction with a 10-m x 30-m grid resolution, respectively (Figure 19). Two bathymetries are set up: a flat bottom with 1-m depth and a sloping bottom with 2.5-m offshore and 0.05 m at the shoreline. When present, tidal currents are assumed to be primarily in shore-parallel direction with a maximum magnitude of about 20 cm/sec. Tidal currents are simulated by imposing flux boundary conditions through the upstream and downstream boundaries of the domain at semi-diurnal frequency. A 4-s sinusoidal wave enters the domain from the offshore boundary with wave heights varying between 0.1 and 0.4 m, at an incident angle of either 0 deg (Scenarios 1-3) or 10 deg (Scenario 4) counterclockwise from the shore-normal direction. The domain of the sediment module is smaller than the entire SHORECIRC/REFDIF domain to avoid anomalous physical forcing near the boundaries, and a looping boundary condition is applied in the shore- parallel direction so that the sediment flux leaving one end of the domain equals the flux entering the other end of the domain. Bottom sediments are initialized with B = 3 kg/m^2 uniformly distributed throughout the domain. In addition to the scenarios reported here, the sediment transport module was verified to conserve mass when suspended sediments and bottom sediments were totaled.

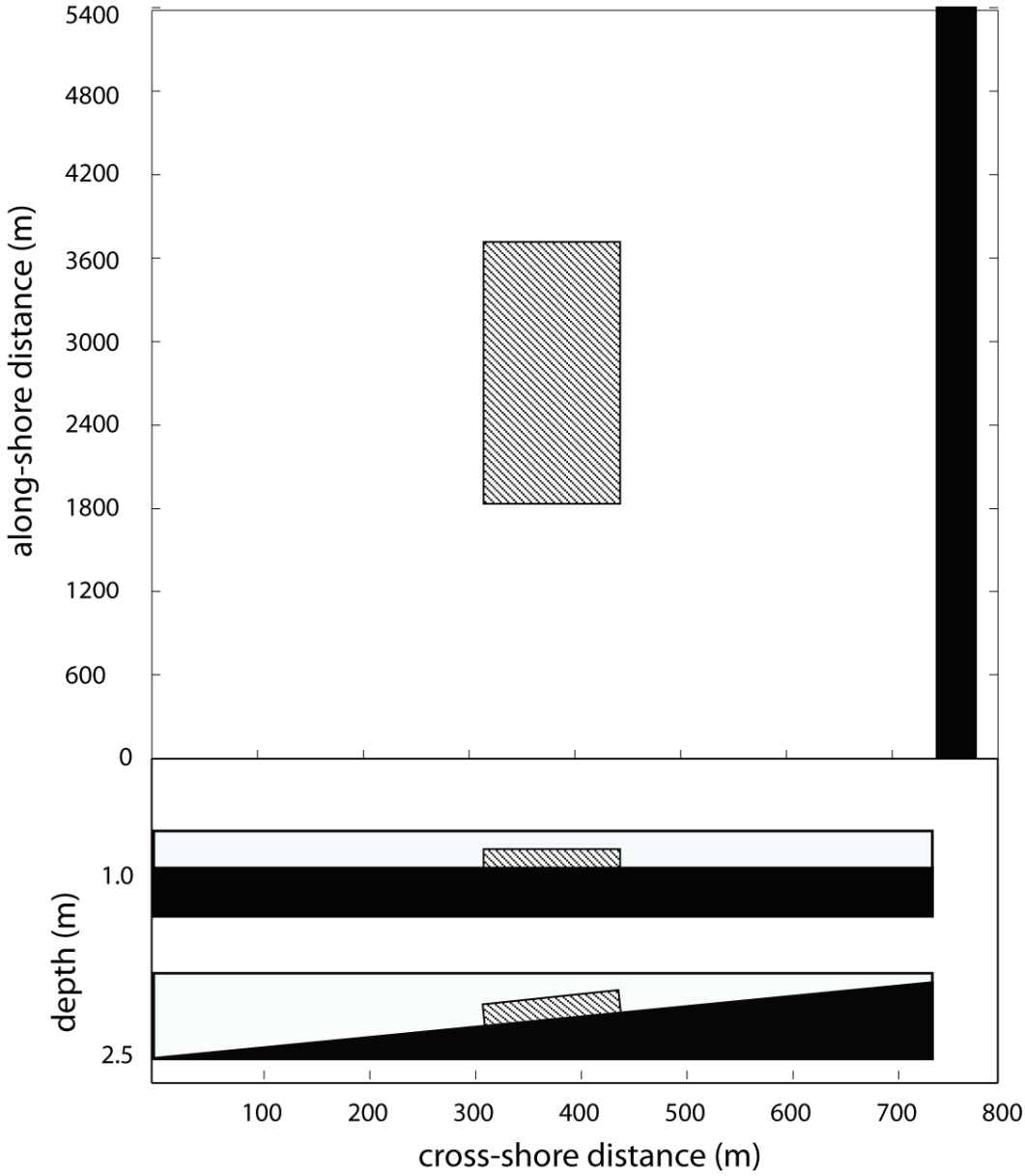

Figure 19. Model domain (top view) and two bathymetries (side view) for model scenarios described in Table 2. The domain is 720 m in cross-shore direction and 5,400 m in along-shore direction with a 10-m x 30-m rectangular grid. The bathymetry with constant depth (1-m) is used in Scenarios 1 to 3, and the sloping bottom with 2.5-m offshore depth and 0.05-m onshore depth is used in Scenario 4.

Table 2. Model scenarios.

Scenario	Bathymetry	Cross-shore Bed Width (m)	Along-shore Bed Length (m)	Position	Physical Forcings	Output Quantities
1	Flat (1 m)	0 to 700 (50m interval)	Full along-shore domain	Offshore edge of bed fixed at off-shore boundary	0.1 to 0.4 m waves, 4 sec, inci-dent angle = 0 (shore-normal)	% of wave energy flux re-duction
2	Flat (1 m)	100	300 to full along-shore domain (300m interval)	Offshore edge of bed fixed at off-shore boundary; Center of bed fixed at the center of along-shore domain	Same as above	Same as above
3	Flat (1 m)	100	Full along-shore domain	Center of bed located 50 to 650 m from off-shore boundary (50-m interval)	Same as above	% of total bottom stress reduction
4	Sloping (2.5m off-shore, 0.05m on-shore)	0	0		0.1 m, 4 sec waves, angle = 10; alongshore tides	Wave height and skin friction shear stress
		200	1800	Center of bed located 550 m from offshore boundary	Same as above	Same as above
		Full cross-shore domain	1800	Center of bed located 360 m from offshore boundary	Same as above	Same as above

The seagrass parameters observed in June for *R. maritima* are applied (density is 1,270/m²; shoot height is 1 m). The circulation, wave, and sediment modules are turned on in all scenarios, and we look at several output quantities. For the first two scenarios, the output quantity is the percentage of wave energy flux reduction. Wave energy flux (F) is the rate at which wave energy is transported in the horizontal direction and can be expressed as:

$$F = EC_g = (\frac{1}{8}\rho g H^2)C_g \quad (36)$$

where E is the wave energy density, C_g is group velocity, ρ is water density, g is the gravitational constant, and H is wave height. In these two scenarios the geometry of the seagrass bed is changed and the ratio of F is calculated with and without seagrasses, averaged over the entire shoreline. The percentage of wave energy flux reduction is then $(1\text{-}F_{with}/F_{without})$ x 100. For the third scenario, the output quantity is the percentage of total bottom stress reduction. Because we are interested in the influences of the seagrass bed on the total force acting on the bottom sediments in the domain, the total bottom stress is defined as the skin friction shear stress integrated over the whole domain. The ratio of total bottom stress with and without the seagrass bed is used to calculate the percentage reduction. In the third scenario, the percent bottom stress reduction is compared as the midpoint of the bed is moved from an inshore position toward the offshore boundary, with bed width and length fixed. The last scenario (sloping bottom) is more realistic than the constant depth scenarios, and the model outputs are examined in more detail. Changes are examined in wave height, skin friction shear stress, suspended sediment, and bottom sediment over both space and time through two tidal cycles. Figure 20 shows changes in wave energy flux reduction when the cross-shore bed width is varied but the bed occupies the entire domain in the along-shore direction (Scenario 1).

The results are presented with respect to only the cross-shore direction, since there is no alongshore variation. Wave energy flux reduction increases with cross-shore coverage but levels off as complete coverage is approached. The increase in energy flux reduction is obviously due to the increase in seagrass wave drag as the bed becomes wider. The energy flux reduction levels off at high percent coverage simply because not much wave energy is left to dissipate, so the rate of change decreases. Expressed

mathematically using linear wave theory, the variation of wave energy flux can be written as:

$$\frac{dF}{dx} = -\varepsilon = -\frac{\rho f}{6\pi}\left(\frac{0.5H\omega}{kh}\right)^3 \tag{37}$$

where ε is energy dissipation rate, f is wave friction factor, ω is angular frequency, k is wave number, h is water depth, and x is distance across-shore. Percent energy flux reduction increases with increasing wave height because a larger wave height exerts a higher stress on the bottom, proportional to the wave orbital velocity squared. The wave energy dissipation rate is proportional to the product of stress and wave orbital velocity for rough turbulent flow (Dean and Dalrymple 1991), so wave energy dissipation is proportional to orbital velocity (thus wave height) cubed, while wave energy flux is only proportional to wave height squared. Thus, wave energy dissipation is proportionately more effective for higher waves.

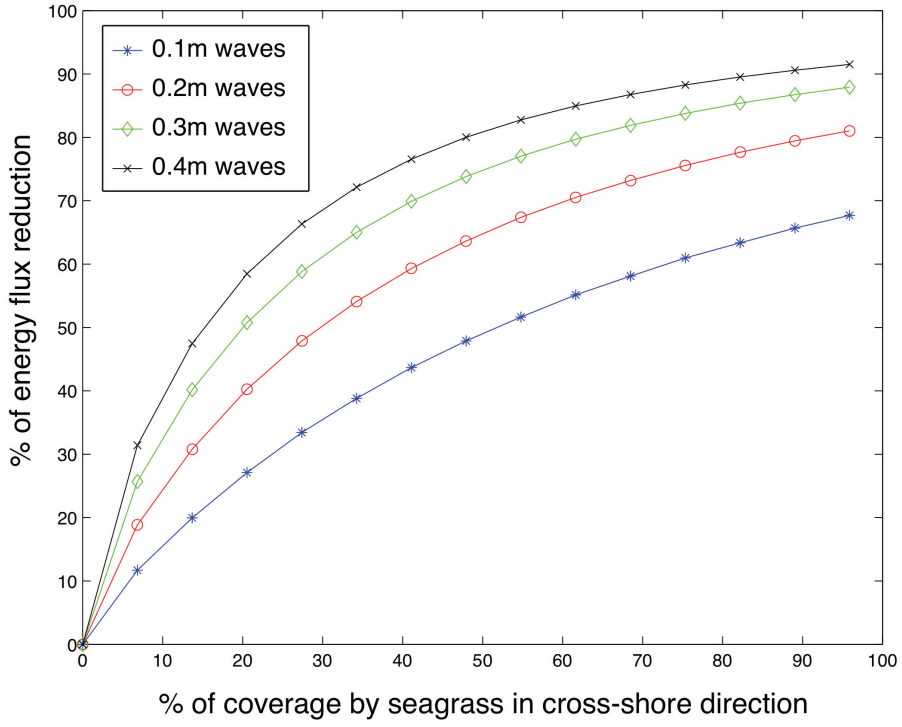

Figure 20. Changes in wave energy flux reduction (indicator of wave attenuation) at the shoreline when the cross-shore coverage of the seagrass bed increases (see Scenario 1 in Table 2 for details). Four different incident wave heights (0.1 to 0.4 m) are applied and represented by different symbols (star, circle, diamond, and cross). Incident waves are shore-normal direction.

Figure 21 shows changes in wave energy flux reduction for Scenario 2, in which the alongshore coverage of the bed is changed while keeping the cross-shore coverage fixed. As expected, wave energy flux reduction is linearly proportional to the alongshore seagrass coverage. Again, percent energy flux reduction increases with incoming wave height.

Figure 22 presents the percent reduction in total force acting on bottom sediments as the position of the bed is moved from inshore towards the offshore boundary (Scenario 3), with a fixed bed width of 100 m and length covering the whole domain in the alongshore direction.

It can be seen that total bottom stress reduction increases approximately linearly with the offshore distance of the bed. It makes sense that the total force acting on bottom sediments is reduced by moving the bed offshore because the affected area between the bed and shoreline increases linearly with the distance of the bed offshore. The smaller waves that emerge from the seagrass bed act over this entire area. Again, larger waves result in proportionately higher bottom stress reduction.

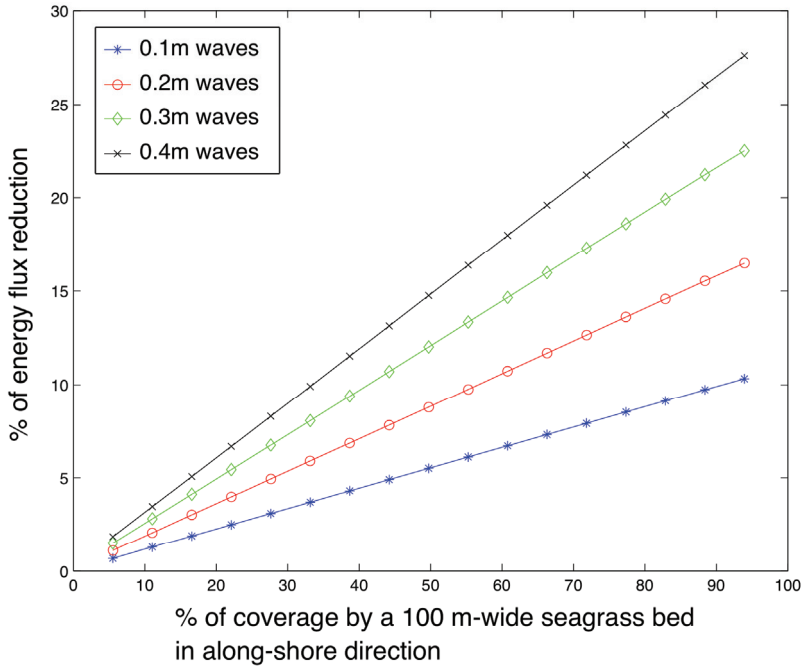

Figure 21. Changes in wave energy flux reduction at the shoreline when the alongshore coverage of the seagrass bed increases with fixed cross-shore coverage (Scenario 2). Four different incident wave heights (0.1 to 0.4 m) are applied and represented by different symbols. Incident waves are shore-normal.

For the fourth scenario, the more realistic sloping bottom case, comparisons are made of model runs with no seagrass, a seagrass bed 200 m wide and 1,800 m long, and a seagrass bed that covers the entire width of the domain and is 1,800 m long. Figure 23 shows across-shore transects of wave height and skin friction shear stress across the center of the seagrass bed at slack tide. In Figure 23a, wave shoaling and then breaking as waves propagate shoreward can be seen without the seagrass bed. This wave height evolution corresponds to the increase and quick drop of skin friction shear stress shown in Figure 23b. In both cases with seagrass beds, wave height and skin friction shear stress within and behind the bed are greatly reduced. The breaking zone and the peak of skin friction shear stress for the case with a 200-m-wide bed are moved shoreward. When the cross-shore domain is fully occupied by the seagrass bed, the breaking zone disappears. Differences between all three cases in deeper water near the offshore boundary are relatively small. The reason is that short period wave orbital velocity decays with depth, making bottom friction less effective to dissipate wave energy in deeper areas. Thus, interactions between seagrass beds and waves in deeper water depend on wave period; longer period waves interact more effectively with seagrass beds in deeper water.

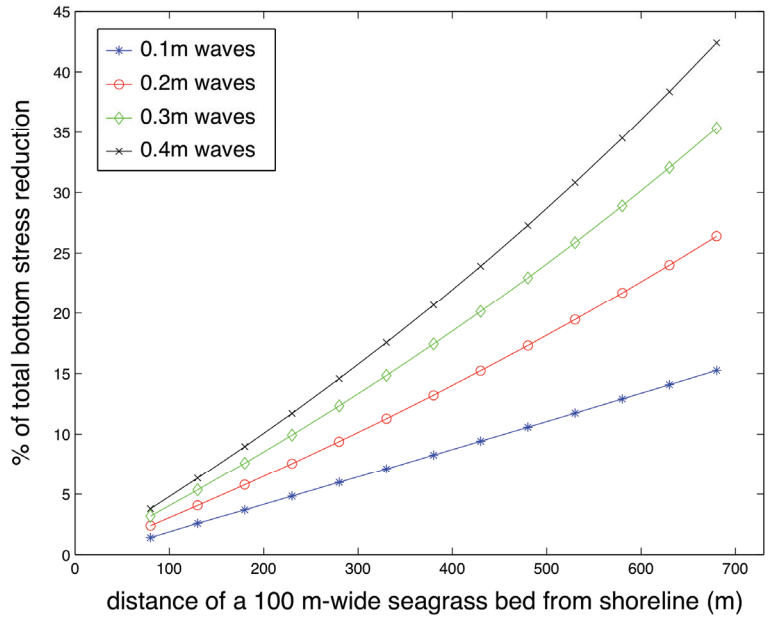

Figure 22. Changes in total bottom stress reduction (indicator of total force acting on bottom sediments) when a seagrass bed with fixed alongshore and cross-shore coverage (100 m wide) is moved offshore (Scenario 3). Four different incident wave heights (0.1 to 0.4 m) are applied and represented by different symbols. Incident waves are shore-normal.

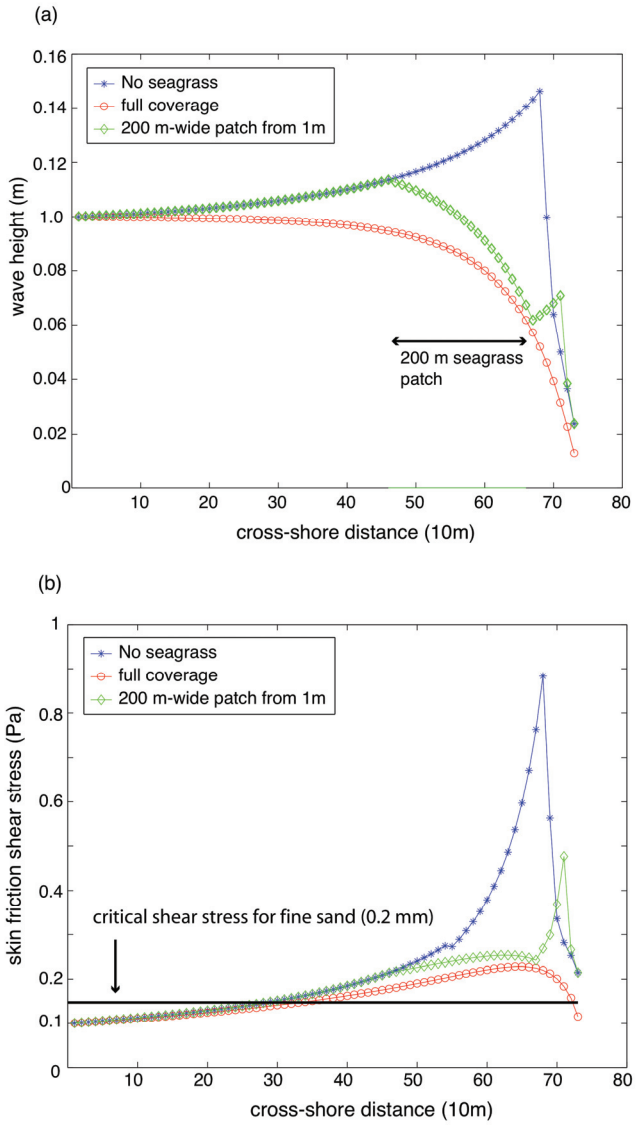

Figure 23. (a) wave height evolution when waves propagate along the central transect from the offshore boundary to shoreline under three seagrass bed configurations: no seagrass (star), full-coverage (circle), and 200-m-wide bed (diamond). The location of 200-m-wide bed is indicated by arrows and is illustrated in Figure 24 (a) by the rectangular box. See Scenario 4 in Table 2 for details. (b) Changes in skin friction shear stress corresponding to wave height evolution with cross-shore distance in (a). The solid line represents the critical shear stress above which fine sands of 0.2 mm diameter start to move.

Reduced skin friction has important implications from the standpoint of sediment transport. To demonstrate this, a line is placed in Figure 23b to indicate the critical shear stress (about 0.15 Pa; U.S. Army Corps of Engineers 2002) for fine sands (0.2 mm). Sediments start to move when shear stress exceeds a critical value (Equation 32). As shown in Figure 23b, the distances over which the critical stress is exceeded are about the same with or without the seagrass beds. However, the erosion rate is proportional to

the distance between the lines of wave-induced skin friction and critical shear stress (Equation 32). Erosion rate is thus greatly reduced within and behind the seagrass beds. This implies that, without advection of sediment from external sources, suspended sediment concentrations within and behind the beds may be lower than those with no seagrass bed. Although greatly simplified, these model results illustrate that realistic bed geometries can have profound effects on waves and can subsequently influence sediment dynamics.

To further examine the effects of seagrass beds on sediment dynamics, the time series is compared of six variables associated with sediments between the 200-m-wide bed case (Figure 24a) and the no seagrass case (Figure 24b) over two full tidal cycles. The variables are bottom sediments, suspended sediment concentration, skin friction shear stress, current magnitude, erosion rate, and deposition rate. In Figure 24, each panel contains three lines that represent the averaged values of each variable offshore of the bed, within the bed (or where the bed would be), and between the bed and the shoreline. As can be seen in Figure 24, current magnitudes show semidiurnal tidal signals and, when the seagrass bed is not present, they decrease shoreward due to increased bottom friction. Current magnitudes at the onshore position during floods are slightly smaller than ebbs because flooding tides are against wave-induced alongshore currents (toward positive y direction). However, when a 200-m-wide bed is added (Figure 24a), current magnitude inside the bed is reduced and becomes smaller than either offshore or onshore.

In the time series of five other variables, tidal signals are weak, especially for shallower locations, indicating that the sediment dynamics in the system are dominated by waves. Most importantly, averaged suspended sediment concentration, skin friction shear stress, erosion rate, and deposition rate are lower and there is more bottom sediment at both the seagrass bed and onshore positions when the seagrass bed is present. This result confirms the anticipation of lower suspended sediment concentration from Figure 23 and suggests that seagrass beds can protect bottom sediments from being eroded not only inside the bed itself but also the area behind it.

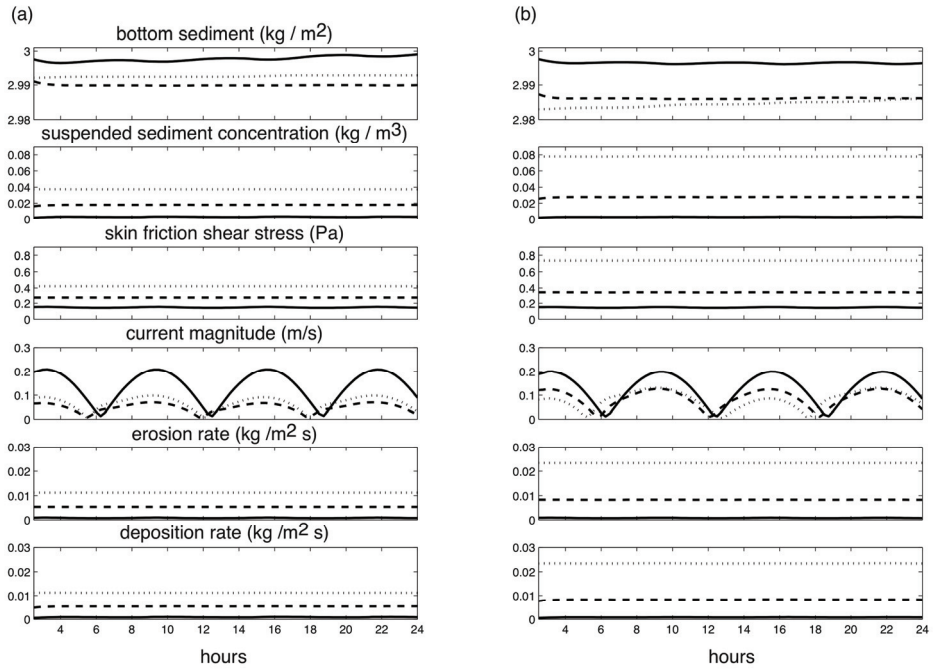

Figure 24. Time series of six variables for the configuration of 200 m-wide bed (a) and no-seagrass (b), as described in Scenario 4. The variables are bottom sediments (kg/m²), suspended sediment concentration (kg/m³), skin friction shear stress (Pa), magnitude of current (m/s), erosion rate (kg/m²s), and deposition rate (kg/m²s) from the top to bottom panel. The time series are collected along the central transect, as shown in solid shore-normal line in Figure 24 (a). The solid line here represents average of each variable from the offshore boundary to the offshore edge of the bed (450 m from offshore boundary); the dashed line is the average within the bed (from 450 to 650 m); the dotted line is the average over the rest of the domain.

Figure 25 shows a snapshot of distributions of suspended (lower panels) and bottom sediments (upper panels) with and without the seagrass bed at maximum flood. For the no-seagrass case (Figure 25b), suspended sediment concentration increases shoreward with little alongshore variation, causing bottom sediments to decrease. This pattern again indicates the dominance of wave-induced erosion. Adding a 200-m-wide seagrass bed induces both alongshore and cross-shore variations of suspended and bottom sediment distributions, as can be seen in Figure 25a. Due to higher drag of the bed, tidal currents are forced to flow around it, resulting in a bulge of suspended sediments at the upstream offshore corner of the bed. A similar pattern is observed at the downstream offshore corner when tides change direction. In general, suspended sediment concentration within the bed is lower than that either onshore or offshore, but advection of suspended sediments by tidal currents can locally increase the concentration within the bed. As for bottom sediments, local scouring is evident at the corners of the bed on the nearshore side. The scouring could be due

to enhanced tidal flow speed between the shoreline and the bed. However, field observations could not be found to support such scouring in the literature and suspect that this effect may be exaggerated by the wall boundary condition in the model. Besides, there are generally more bottom sediments within the bed than on either side, mostly near the upper and lower edges. The sediment trapping is due to import of higher suspended sediment concentration by tidal currents from outside, deposition of these sediments, and lower wave-induced erosion rates inside.

Animating the model results confirms that sediment trapping appears to occur at the upstream edge on each half tidal cycle, when tidal currents are advecting higher suspended sediment concentrations from outside into the seagrass bed.

Implications and utility of modeling studies

Wave attenuation by seagrass beds

Several general statements can be made from the results of the model scenarios with a flat bottom (Figures 20-22). First, larger coverage of seagrasses in the direction of wave propagation results in higher wave attenuation (indicated by percent of energy flux reduction) and thus less energy reaching the shoreline. Second, the total force acting on the bottom (indicated by percent of bottom stress reduction) over the whole domain decreases as the seagrass bed is moved offshore. Third, relative wave attenuation and bottom stress reduction are greater for larger incoming wave heights.

These statements are generally valid as long as there is significant interaction between wave orbital velocities and the seagrass canopy. This qualification may be interpreted as a generalization of suggestions by Ward et al. (1984) and Koch (2001). They pointed out that wave attenuation should be higher when seagrass occupies a large portion of the water column. Indeed, for our flat bottom cases, seagrass shoots occupied the entire water column (June case), and the decay of orbital velocity with depth was negligible (at 1-m depth, 4 sec waves are close to shallow-water waves). In contrast, in our sloping bottom cases 1-m seagrass shoots only occupied part of the water column in the deepest region (2.5-m depth), and orbital velocity decayed at least 25 percent. This is why the differences in wave height between no-seagrass and full-coverage cases (Figure 8a) are relatively small in the deepest region but increase in shallower regions. Although a

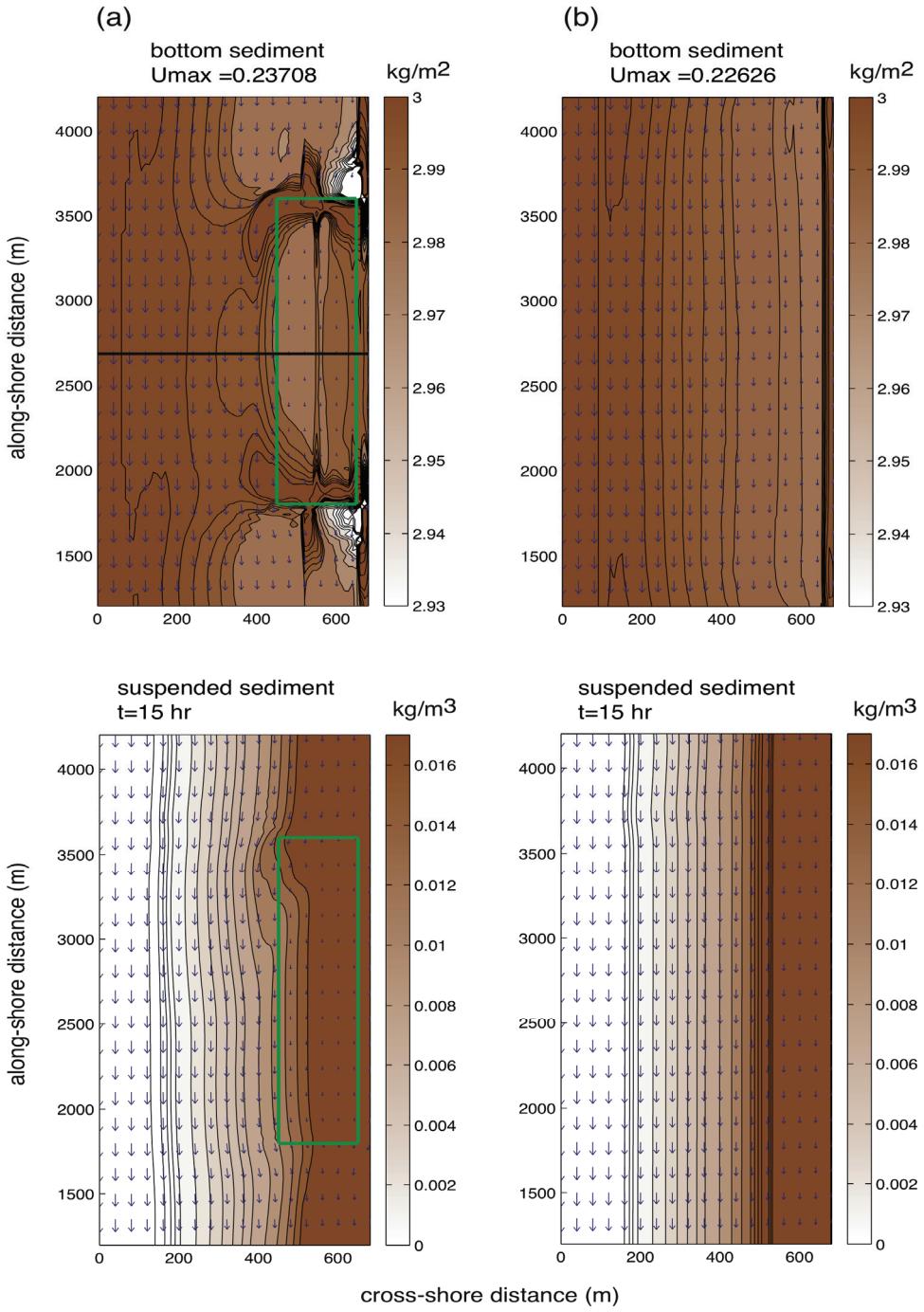

Figure 25. Snapshot (top view of model domain) of distribution of bottom sediments (upper panel) and suspended sediment concentration (bottom panel) for the configuration of 200-m-wide bed (a) and no-seagrass (b). The M2 tide is forced in the alongshore direction, while 0.1 m, 4 sec waves propagate from offshore boundary with 10 deg incident angle (counterclockwise from shore-normal direction). The current direction and magnitude are indicated by vectors, and bottom sediment and suspended sediment concentration are shown in contour. The solid line in (a) represents the central transect along which model outputs in Figure 7 and 8 are collected. It should be noted that the alongshore domain (5,400 m) is set smaller than the domain of SHORECIRC / REFDIF, and a looping boundary condition is applied.

flume study (Fonseca and Cahalan 1992) and field observations (Koch 1996) indirectly support this hypothesis, wave attenuation has also been observed when seagrass only occupies a small portion of the water column (Granata et al. 2001; depth of 15 m). Systematic observations on the effects of seagrass bed geometry on waves with different wave heights and periods are needed to verify model predictions and to better understand these processes.

Wave attenuation by seagrass may have implications for shoreline protection (van Katwijk 2000; Koch et al. 2006). Using observed seagrass parameters in June, our model results showed significant reductions in wave energy flux at the shoreline for both flat and sloping bottom cases (Figure 20, 21, and 23). However, seagrasses vary seasonally in temperate environments, whereas shoreline erosion is usually associated with large wave events that occur episodically (Wilcock et al. 1998) over annual or decadal time scales (Kamphuis 1987). Hence, the timing between wave events and seagrass growth influences the potential for seagrass beds to protect shorelines. Without knowing more about this timing, it is difficult to evaluate the net influence of seagrass on shoreline protection based on the results presented here. Other factors such as the spectral or directional distributions of wave energy may also need to be considered in order to better address this question. REF/DIF is capable of modeling spectral wave forcing as well as multiple wave incident angles (Kirby and Tuba Ozkan 1994), closer to what is observed in the field. Those issues will be addressed in the future.

Sediment dynamics

Model results have two main implications for sediment dynamics. First, sedimentary processes are altered within the seagrass bed and probably behind it. Results from Scenario 3 (Figure 22) show that, in wave-dominated environments, the total force acting on bottom sediments decreases as the seagrass bed is moved offshore due to increases in the affected area behind the bed. This suggests that seagrass beds may stabilize bottom sediments in the zone between the bed and shoreline, which is consistent with Hine et al. (1987)'s observation that disappearance of a seagrass community allowed rapid onshore and longshore sand transport in the nearshore zone. Similarly, comparison between cases with and without a 200-m-wide bed (Figure 24) shows lower skin friction shear stresses, lower erosion rates, and higher levels of bottom sediments at locations within and behind the bed. Within the bed, the result is consistent

with Lopez and Garcia (1998)'s findings. Applying a numerical model of open channel flow with simulated vegetation, they showed reduced shear stress and consequently lower suspended sediment transport (partly due to lower suspended sediment concentration) in the vegetated area. Reduced erosion rate as well as bottom sediment retention are also supported by field observations (Gacia and Duarte 2001). Gacia and Duarte found that the presence of *Posidonia oceanica* enhances sediment stability by preventing resuspension. Behind the bed, however, there is no quantitative evidence to support the model-predicted reduction in skin friction shear stress and erosion and sediment retention. Further studies are required for verification.

Second, sediment trapping in the seagrass bed requires horizontal transport to bring suspended sediment from outside into the bed. The concept of a seagrass bed as a depositional environment has been suggested by several authors (e.g., Grady 1981; Ward et al. 1984; Almasi et al. 1987), and the proposed mechanism for this accumulation may be summarized as reduced shear stress due to loss of momentum in a seagrass bed leading to reduction in resuspension and thus increased sediment accumulation (Koch et al. 2006). The connection between lower momentum and reduced resuspension (lower erosion rate) is supported by our results. However, the results suggest that linkages from reduced resuspension to increased accumulation are not trivial and may not occur everywhere within the bed. Sediment accumulation occurs when the suspended sediment concentration is high enough that the deposition rate exceeds the erosion rate. Sediment accumulation at the upper and lower edges of the bed in Figure 25a illustrates this point. At these two edges, accumulation occurs when high concentrations of suspended sediment from outside are transported into the bed, where reduced shear stresses allow them to deposit. The amount of accumulated sediment then gradually decreases with distance into the bed until the sediment source from outside is used up. Beyond this location, sediments that were originally there remain, but there is no new accumulation.

In short, the model results clearly demonstrate that sediment accumulation requires both sediment sources (outside the bed) and a transport mechanism (tidal currents), both of which may vary spatially within the bed. The reduction in suspended sediment transport capacity (concentration multiplied by streamwise velocity) in a vegetated area reported by Lopez and Garcia (1998) indirectly supports accumulation at the bed edge.

Nevertheless, direct observations of spatial patterns of accumulation within seagrass beds are few, and most of them focus on sediment grain size distributions (e.g., Scoffin 1970; Wanless 1981; Granata et al. 2001). More observations that can resolve spatial patterns of erosion/deposition are needed to move our understanding forward. It should also be noted that the spatial distribution of bottom sediment presented here may not match field observations exactly because these model scenarios do not account for limited supplies of surficial sediments or mixed sediment grain sizes.

Utility of modeling studies

Teeter et al. (2001) summarized the complexities of modeling interactions between waves, flow, and sediment transport in seagrass beds quite clearly, and pointed out some of the limitations in our current capabilities. The model presented here underscores the importance of adequately representing these complex interactions. For example, it is quite clear from the model runs that wave forcing alone will not result in enhanced deposition within a seagrass bed. Wave forcing can create an erosional environment outside and a depositional environment inside, but without currents forced by winds or tides, there will be little transport of suspended sediment from outside to inside. It is important to point out that our model in fact does not represent all of the potential interactions identified by Teeter et al. (2001), ignoring direct wind forcing, multiple sediment grain sizes, and large tidal height variability; and neither the framework presented by Teeter et al. nor the present model consider ecosystem effects (such as feedbacks to seagrass growth).

Given the complexities of these interactions, the uncertainties associated with attempting to model some of them, and the daunting task of developing and successfully implementing the equally complex computer codes required, it might be asked if the effort is justified. The answer from our point of view is a resounding "yes," but not in isolation. We hope that some of the example scenarios presented here have illustrated the utility of the modeling approach, especially in combination with sparse data. The primary advantages of modeling are:

a. To generate testable hypotheses or to help explain observations. For example, the model that was presented predicts that sediment deposition in seagrass beds should be most pronounced just inside the bed on the upstream side, and that internal gradients in deposi-

tion will be quite large. Is this observable? The model also predicts that wave attenuation expressed as a percentage of the incoming wave energy will be greater for higher waves, which is apparent qualitatively in data presented elsewhere in this report.

b. To aid in the design of observational programs or restoration efforts. From an experimental design perspective, given reasonable estimates of tidal currents, waves, seagrass densities, and bed sizes, a model might be used to anticipate where sparse instrumentation could be put to best use, and what kind of measurements might be expected to yield the most useful observations. From a restoration point of view, if the goal is to use seagrass beds to reduce nearshore turbidity due to resuspension, Figure 22 indicates that a bed placed further offshore will have a greater effect on total bottom stress reduction (hence, total resuspension) - that is, unless the bed is also so deep that it falls below wave base and no longer affects the waves. However, the bed distance offshore has relatively little predicted impact on reduction in wave power striking the shoreline (not shown).

c. To help interpolate sparse data in space and time. We can never measure enough to cover all scales of interest and all times, but if we can measure enough to build and parameterize a reliable model, we can fill in the gaps.

For these reasons, we advocate the development and use of numerical models in conjunction with careful field and laboratory measurements as the best possible combination of tools to address both research and restoration goals.

7 Summary and Conclusions

While extensive work has been done on how currents move through seagrass beds, how currents are affected by seagrasses and how seagrasses are affected by currents, our understanding about how waves propagate through seagrass beds, are affected by seagrasses and affect seagrass biology is still in its infancy. It has been just recently that more attention has been paid to this field of study. By using experimental designs and instrumentation that allows for easy comparison between studies, it will be possible to gather the information so much needed to understand waves in vegetated systems. The continuous development of smaller electronics now also allows for the deployment of wave sensors in relatively shallow waters. Modeling of waves in seagrass colonized areas has also seen a tremendous leap in recent years but many questions still remain to be explored. The continuous and careful collection of field and lab data on waves in seagrass beds of different species, at different depths and at different times of the year will allow existing models to be refined and new models to be developed. In summary, wave-related processes in seagrass systems is a fascinating field in which extensive contributions can still be made.

References

Ackerman, J. D., and A. Okubo. 1993. Reduced mixing in a marine macrophyte canopy. *Functional Ecology* 7:305-309.

Almasi, M. N., C. M. Hoskin, J. K. Reed, and J. Milo. 1987. Effects of natural and artificial Thalassia on rates of sedimentation. *Journal of Sedimentary Petrology* 57:901-906.

Bell, S. S., M. S. Fonseca, and L. B. Mooten. 1997. Linking restoration and landscape ecology. *Restoration Ecology* 5:318-323

Bishop, C. T., and M. A. Donelan. 1987. Measuring waves with pressure transducers. *Coastal Engineering* 11:309-328.

Bokaian, A., and F. Geoola. 1984. Wake-induced galloping of two interfering circular cylinders. *Journal of Fluid Mechanics* 146:383-415.

Bridgwood, S. D. 2002. The structure and function of windrows in meadows of the seagrass *Posidonia sinuosa*. Honours thesis, Murdoch University.

Campbell, M. L., and E. I. Paling. 2003. Evaluating vegetative transplant success in *Posidonia australis*: A field trial with habitat enhancement. *Marine Pollution Bulletin* 46:828-834.

Chiscano, C. L. 2000. The effect of wave exposure on submersed aquatic vegetation. MS thesis, University of Maryland, College Park, 145 pp.

Clarke, S., and A. J. Elliott. 1998. Modelling suspended sediment concentration in the firth of forth. *Estuarine Coastal and Shelf Science* 47:235-250.

Costanza, R., R. d'Arge, R. de Groot, S. Farber, M. Grasso, B. Hannon, S. Naeem, K. Limburg, J. Paruelo, R. V. O'Neill, R. Raskin, P. Sutton, and M. van den Belt. 1997. The value of the world's ecosystem services and natural capital. *Nature* 387:253-260.

Dan, A., A. Moriguchi, K. Mitsuhashi, and T. Terawaki. 1998. Relationship between *Zostera marina* beds and bottom sediments, wave action offshore in Naruto, southern Japan (original title: Naruto chisaki ni okeru amamo-ba to teishitsu oyobi haro tono kankei). *Fisheries Engineering* (Japan)/Suisan Kogaku (Japan) 34:299-304.

Dean, R. G., and R. A. Dalrymple. 1991. *Water wave mechanics for engineers and scientists*. World Scientific.

Denman, K. L. 1975. *Spectral analysis: A summary of the theory and techniques*. Technical Report Number 539 from the Fisheries and Marine Service, Canada, 28 pp.

Dennison, W. C., R. J. Orth, K. A. Moore, J. C. Stevenson, V. Carter, S. Kollar, P. W. Bergstrom, and R. A. Batiuk. 1993. Assessing water quality with submersed aquatic vegetation. *BioScience* 43:86-94.

Dromgoole, F. I. 1988. Light fluctuations and photosynthesis in marine algae. 2. Photosynthetic response to frequency, phase ratio and amplitude. *Functional Ecology* 2(2), 211-219.

Duarte, C. M. 1991. Seagrass depth limits. *Aquatic Botany* 40: 363-377.

Edgar, G. J., and C. Shaw. 1991. Inter-relationships between sediment, seagrasses, benthic invertebrates and fishes in shallow marine habitats off South-Western Australia. *The Marine Flora and Fauna of Rottnest Island, Western Australia. Western Australian Museum, Perth, Western Australia*, 429-442.

Finnigan, J. 2000. Turbulence in plant canopies. *Annual Review of Fluid Mechanics* 32:519-571.

Fonseca, M. S. 1996. The role of seagrasses in nearshore sedimentary processes a review. In *Estuarine shores: Evolution environments and human alterations*. K. F. Nordstrom and C. T. Roman, ed., 261-286. John Wiley and Sons Ltd.

Fonseca, M. S. 1998. *Exploring the basis of pattern expression in seagrass landscapes*. PhD diss., Department of Integrative Biology, University of California, Berkeley, CA, 222 pp.

Fonseca, M. S., J. S. Fisher, J. C. Zieman, and G. W. Thayer. 1982. Influence of the seagrass *Zostera marina* on current flow. *Estuarine, Coastal and Shelf Science* 15:351-364.

Fonseca, M. S., J. C. Zieman, G. W. Thayer, and J. S. Fisher. 1983. The role of current velocity in structuring seagrass meadows. *Estuarine, Coastal and Shelf Science* 17:367–380.

Fonseca, M. S., and J. S. Fisher. 1986. A comparison of canopy friction and sediment movement between four species if seagrass with reference to their ecology and restoration. *Marine Ecology Progress Series* 29:15-22.

Fonseca, M. S., and W. J. Kenworthy. 1987. Effects of current on photosynthesis and distribution of seagrasses. *Aquatic Botany* 27:59-78.

Fonseca, M. S., and J. A. Cahalan. 1992. A preliminary evaluation of wave attenuation for four species of seagrass. *Estuarine, Coastal and Shelf Science* 35:565-576.

Fonseca, M. S., and S. S. Bell. 1998. Influence of physical setting on seagrass landscapes near Beaufort, North Carolina, USA. *Marine Ecology Progress Series* 171:109-121.

Fonseca, M. S., W. J. Kenworthy, and G. W. Thayer. 1998. *Guidelines for mitigation and restoration of seagrass in the United States and adjacent waters*. NOAA COP/Decision Analysis Series. 222p.

Fonseca, M. S., P. E. Whitfield, N. M. Kelly, and S. S. Bell. 2002. Modeling seagrass landscape pattern and associated ecological attributes. *Ecological Applications* 12:218-237.

Fonseca, M. S., and M. A. R. Koehl. 2006. Flow in seagrass canopies: The influence of patch width. *Estuarine, Coastal and Shelf Science* 67:1-9.

Frederiksen, M., D. Krause-Jensen, M. Holmer and J.S. Laursen. 2004. Spatial and temporal variation in eelgrass (*Zostera marina*) landscapes: Influence of physical setting. *Aquatic Botany* 78:147-165.

Gacia, E., T. C. Granata, and C. M. Duarte. 1999. An approach to the measurement of particle flux and sediment retention within seagrass (*Posidonia oceanica*) meadows. *Aquatic Botany* 65:255-268.

Gacia, E., and C. M. Duarte. 2001. Sediment retention by a Mediterranean *Posidonia oceanica* meadow: The balance between deposition and resuspension. *Estuarine, Coastal and Shelf Science* 52:505-514.

Gallegos, C. L., and W. J. Kenworthy. 1996. Seagrass depth limits in the Indian River Lagoon (Florida, USA): Applicant of a water quality optical mol. *Estuarine, Coastal and Shelf Science* 42:267-288.

Gambi, M. C., A. R. M. Nowell and P. A. Jumars. 1990. Flume observations on flow dynamics in *Zostera marina* (eelgrass) beds. *Marine Ecology Progress Series* 61:159-169

Ghisalberti, M., and H. M. Nepf. 2002. Mixing layers and coherent structures in vegetated aquatic flows. *Journal of Geophysical Research* 107:C2, 10.1029.

Grady, J. R. 1981. Properties of seagrass and sand flat sediments from the intertidal zone of St. Andrew Bay, Florida. *Estuaries* 4:335-344.

Granata, T. C., T. Serra, J. Colomer, X. Casamitjana, C. M. Duarte, and E. Gacia. 2001. Flow and particle distributions in a nearshore meadow before and after a storm. *Marine Ecology Progress Series* 218:95-106.

Grant, W. D., and O. S. Madsen. 1979. Combined wave and current interaction with a rough bottom. *Journal of Geophysical Research-Oceans and Atmospheres* 84: 1797-1808.

Green, E. P., and F. T. Short. 2003. *World atlas of seagrasses*. University of California Press, Berkeley.

Greene, R. M., and V. A. Gerard. 1990. Effects of high-frequency light fluctuations on growth and photoacclimation of the red alga *Chrondrus crispus*. *Marine Biology* 105(20), 337-344.

Grizzle, R. E., F. T. Short, C. R. Newell, H. Hoven, and L. Kindblom. 1996. Hydrodynamically induced synchronous waving of seagrasses: Monami and its possible effects on larval mussel settlement. *Journal of Experimental Marine Biology and Ecology* 206:165-177.

Hemminga, M. A., and C. M. Duarte. 2000. *Seagrass ecology*. Cambridge University Press, Cambridge.

Hine, A. C., M. W. Evans, R. A. Davis, and D. Belknap. 1987. Depositional response to seagrass mortality along a low-energy, barrier-island coast: West-central Florida. *Journal of Sedimentary Petrology* 57(3): 431-439.

Hoskin, C. M. 1983. Sediment in seagrasses near Link Port, Indian River, Florida. *Florida Scientist* 46:153-161.

Hovel, K. A., M. S., Fonseca, D. L. Meyer, W. J. Kenworthy, and P. E. Whitfield. 2002. Effects of seagrass landscape structure, structural complexity and hydrodynamic regime on macroepibenthic faunal densities in North Carolina seagrass beds. *Marine Ecology Progress Series* 243:11-24.

Howell, G. L. 1998. Shallow water directional wave gages using short baseline pressure arrays. *Coastal Engineering* 35:85–102.

Huber, C. 2003. Wave damping effects caused by seagrasses. Diploma thesis, Department of River and Coastal Engineering, Technical University Hamburg-Harburg, Germany, 65 pp.

Johnson, D. 2001. *DIWASP, A directional wave spectra toolbox for MATLAB®: User manual*. Research Report WP-1601-DJ (V1.1), Centre for Water Research, University of Western Australia. http://www.cwr.uwa.edu.au/~johnson/diwasp.diwasp.html.

Jones, C. G., J. H. Lawton, and M. Shachak. 1994. Organisms as ecosystem engineers. *Oikos* 69:373-386.

Jones, C. G., J. H. Lawton, and M. Shachak. 1997. Positive and negative effects of organisms as physical ecosystem engineers. *Ecology* 78:1946-1957.

Kamphuis, J. W. 1987. Recession rate of glacial till bluffs. *Journal of Waterway Port Coastal and Ocean Engineering* 13: 60-73.

Keddy, P.A. 1982. Quantifying within lake gradients of wave energy: Interrelationships of wave energy, substrate particle size and shoreline plants in Axle Lake, Ontario. *Aquatic Botany* 14:41-58.

Kelly, N. M., M. S. Fonseca, and P. E. Whitfield. 2001. Predictive mapping for management of seagrass beds. *Aquatic Conservation: Marine and Freshwater Ecosystems* 11:437-451.

Kemp,W. M., R. Batiuk, R. Bartleson, P. Bergstrom, V. Carter, C. Gallegos, W. Hunley, L. Karrh, E.W. Koch, J. Landwehr, K. Moore, L. Murray, M. Naylor, N. Rybicki, J.C. Stevenson, and D. Wilcox. 2004. Habitat requirements for submerged aquatic vegetation in Chesapeake Bay: Water quality, light regime, and physical-chemical factors. *Estuaries* 27(3):363-377.

Kendrick, G. A., B. J. Hegge, A. Wyllie, A. Davidson, and D. A. Lord. 2000. Changes in seagrass cover on Success and Parmelia Banks, Western Australia between 1965 and 1995. *Estuarine Coastal and Shelf Science* 50:341-353.

Kenworthy, W. J., and M. S. Fonseca. 1996. Estimating the relationship between distribution and light requirements for the seagrasses *Syringodium filiforme* and *Halodule wrightii*. *Estuaries* 19:740-750.

Kenworthy, W. J., J. C. Zieman, and G. W. Thayer. 1982. Evidence for the influence of seagrasses on the benthic nitrogen cycle in a coastal plain estuary near Beaufort, North Carolina (USA). *Oecologia* 54:152-158.

Kirby, J.T., and R. A. Dalrymple. 1994. *Combined refraction / diffraction model, REF/DIF 1, Version 2.5, Documentation and User's Manual, Center for Applied Coastal Research*. University of Delaware, Newark.

Kirby, J. T., and H. Tuba Ozkan. 1994. *Combined refraction / diffraction model for spectral wave conditions, REF/DIF S, Version 1.1, Documentation and user's manual.* Center for Applied Coastal Research. University of Delaware, Newark.

Kirkman, H., and J. Kuo. 1990. Pattern and process in southern Western Australian seagrasses. *Aquatic Botany* 37:367-382.

Kobayashi, N., A. W. Raichle, and T. Asano. 1993. Wave attenuation by vegetation. *Journal of Waterway Port Coastal and Ocean Engineering* 119(1):30-48.

Koch, E. W. 1993. *Hydrodynamics of flow through seagrass canopies.* PhD diss, University of South Florida, St. Petersburg, FL, 123 pp.

Koch, E. W. 1994. Hydrodynamics, diffusion boundary layers and photosynthesis of the seagrasses *Thalassia testudinum* and *Cymodocea nodosa*. *Marine Biology* 18:767-776.

Koch, E. W. 1996. Hydrodynamics of a shallow *Thalassia testudinum* bed in Florida, USA. In *Seagrass Biology – Proceedings of an International Workshop, Western Australia Museum, Perth, Australia*. J. Kuo, R. C. Phillips, D. I. Walker and H. Kirkman, ed., 105-110.

Koch, E. W. 1999. Sediment resuspension in a shallow Thalassia testudinum bed. *Aquatic Botany* 65:269-280.

Koch, E. W. 2001. Beyond light: Physical, geological and geochemical parameters as possible submersed aquatic vegetation habitat requirements. *Estuaries* 24:1-17.

Koch, E. W. 2002. The impact of boat-generated waves on a seagrass habitat. *Journal of Coastal Research* 37:66-74.

Koch (in preparation). *Wave exposure: An additional SAV habitat requirement in the Chesapeake Bay*.

Koch (unpublished). *Do oyster filtration and wave attenuation associated with oyster reefs and breakwaters improve seagrass habitat?* A project funded by Maryland SeaGrant.

Koch, E. W., and G. Gust. 1999. Water flow in tide- and wave-dominated beds of the seagrass *Thalassia testudinum*. *Marine Ecology Progress Series* 184:63-72.

Koch, E.W., J. Ackerman, M. van Keulen, and J. Verduin. 2006. Fluid dynamics in seagrass ecology: from molecules to ecosystems. In *Seagrasses: Biology, ecology and conservation*. A. W. D. Larkum, R. J. Orth and C. M. Duarte, ed. Springer Verlag, 193-225.

Koch, E.W., and J. Verduin. 2001. Measurements of physical parameters in seagrass habitats. In *Global seagrass research methods*. F. T. Short and R.G. Coles, ed. Elsevier Science, Amsterdam, 325-344.

Koehl, M. A. R. 1984. How do benthic organisms withstand moving water? *Amer. Zool.* 24:57-70.

Kopp, B. S. 1999. *Effects of nitrate fertilization and shading on physiological and biomechanical properties of eelgrasss* (Zostera marina*)*. Ph.D. diss., University of Rhode Island, 187 pp.

Krause-Jensen, D., M. F. Pedersen, and C. Jensen. 2003. Regulation of eelgrass (*Zostera marina*) cover along depth gradients in Danish coastal waters. *Estuaries* 26:866-877.

Kundu, P. K., and I. M. Cohen. 2002. *Fluid mechanics*, 2nd edition, San Diego, CA: Academic Press.

Leonard, B. P. 1979. Stable and accurate convective modeling procedure based on quadratic upstream interpolation. *Computer Methods in Applied Mechanics and Engineering* 19: 59-98.

Lopez, F., and M. Garcia. 1998. Open-channel flow through simulated vegetation: suspended sediment transport modeling. *Water Resources Research* 34:2341-2352.

Martin, D., F. Bertasi, M. A. Colangelo, M. de Vries, M. Frost, S. J. Hawkins, E. Macpherson, P. S. Moschella, M. P. Satta, R. C. Thompson, and V. U. Ceccherelli. 2005. Ecological impact of coastal defense structures on sediment and mobile fauna: Evaluating and forecasting consequences of unavoidable modifications of native habitats. *Coastal Engineering* 52:1027-1051.

Marbà, N., J. Cebrian, S. Enriquez, and C. M. Duarte. 1994. Migration of large-scale subaqueous bedforms measured with seagrasses (*Cymodocea nodosa*) as tracers. *Limnology and Oceanography* 39:126-133.

Mendez, F. J., and I. J. Losada. 2004. An empirical model to estimate the propagation of random breaking and non-breaking waves over vegetation fields. *Coastal Engineering* 51: 103-118.

Mendez, F. J., I. J. Losada, and M. A. Losada. 1999. Hydrodynamics induced by wind waves in a vegetation field. *Journal of Geophysical Research-Oceans* 104: 18383-18396.

Middelboe, A. L., K. Sand-Jensen, and D. Frause-Jensen. 2003. Spatial and interannual variations with depth in eelgrass populations. *Journal of Experimental Biology and Ecology* 291:1-15.

Mills, K. E., and M. S. Fonseca. 2003. Mortality and productivity of eelgrass *Zostera marina* under conditions of experimental burial with two sediment types. *Marine Ecology Progress Series* 255:127-134.

Moore, K. A., R. K.Wetzel, and R. J. Orth. 1997. Seasonal pulses of turbidity and their relations to eelgrass (*Zostera marina* L.) survival in an estuary. *Journal of Experimental Marine Biology and Ecology* 215:115-134.

Morgan, P. 2000. *Conservation and ecology of fringing salt marshes in New Hampshire and Maine*. University of New Hampshire. PhD diss., Durham, NH.

Murphey, P. L., and M. S. Fonseca. 1995. Role of high and low energy seagrass beds as nursery areas for Penaeus duorarum in North Carolina. *Marine Ecology Progress Series* 121:91-98.

Nepf, H. M. 1999. Drag, turbulence and diffusion in flow through emergent vegetation. *Water Resources Research* 35: 479-489.

Newell, R. I. E., and E. M. Koch. 2004. Modeling seagrass density and distribution in response to changes in turbidity stemming from bivalve filtration and seagrass sediment stabilization. *Estuaries* 27:793-806.

Nikora, V. I., D. G. Goring, and B. J. F. Biggs. 2002. Some observations of the effect of micro-organisms growing on the bed of an open channel on the turbulence properties. *Journal of Fluid Mechanics* 450:317-341.

North, E. W., S. Y. Chao, L. P. Sanford, and R. R. Hood. 2004. The influence of wind and river pulses on an estuarine turbidity maximum: Numerical studies and field observations in Chesapeake Bay. *Estuaries* 27: 132-146.

Ota, T., N. Kobayashi, and J. T. Kirby. 2004. Wave and current interactions with vegetation. *Proceedings of 29th International Conference on Coastal Engineering, Lisbon, September*, 508-520.

Paling, E. I., M. van Keulen, and K. D. Wheeler. 2003. The influence of spacing on mechanically transplanted seagrass survival in a high energy regime. *Restoration Ecology* 11:56-61.

Patterson, M. R., M. C. Harwell, L. M. Orth, and R. J. Orth. 2001. Biomechanical properties of reproductive shoots of eelgrass. *Aquatic Botany* 69:27-40.

Peterson, C. H., R. A. Luettich Jr., F. Michelli, and G. A. Skilleter. 2004. Attenuation of water flow inside seagrass canopies of differing structure. *Marine Ecology Progress Series* 268:81-92.

Phillips, R. C. 1980. Responses of transplanted and indigenous *Thalassia testudinum* and *Halodule wrightii* to sediment loading and cold stress. *Contributions in Marine Science* 23:79-87.

Pinckney, J. L., and F. Micheli. 1998. Microalgae on seagrass mimics: Does epiphyte community structure differ from live seagrasses? *Journal of Experimental Marine Biology and Ecology* 221:59-70.

Prager, E. J., and R. B. Halley. 1999. The influence of seagrass on shell layers and Florida Bay mudbanks. *Journal of Coastal Research* 15:1151-1162.

Raupach, M. R., A. R. Antonia, and S. Rajagopalan. 1991. Rough-wall turbulent boundary layers. *Applied Mechanics Review* 44:1-25.

Robbins, B. D. and S. S. Bell. 2000. Dynamics of a subtidal seagrass landscape: Seasonal and annual change in relation to water depth. *Ecology* 81:1193-1205.

Robbins, B. D., M.S. Fonseca, P. E. Whitfield, and P. Clinton. 2001. Use of a wave exposure technique for predicting distribution and ecological characteristics of seagrass ecosystems. In *Proceedings: Seagrass management: It's not just nutrients, October 6, 2000*. H. S. Greening, ed., 171-176. Tampa Bay National Estuarine Program, St. Petersburg, FL.

Ruuskanen, A., S. Bäck, and T. Reitalu. 1999. A comparison of two cartographic exposure methods using Fucus vesiculosus as an indicator. *Marine Biology* 134:139-145.

Sanford, L. P., S. E. Suttles, and J. P. Halka. 2001. Reconsidering the physics of the Chesapeake Bay estuarine turbidity maximum. *Estuaries* 24: 655-669.

Scoffin, T. P. 1970. The trapping and binding of subtidal carbonate sediments by marine vegetation in Bimini Lagoon, Bahamas. *Journal of Sedimentary Petrology* 40: 249-273.

Shi, F., I. A. Svendsen, J. T. Kirby, and J. M. Smith. 2003. A curvilinear version of a Quasi-3D nearshore circulation model. *Coastal Engineering* 49: 99-124.

Shore protection manual. 1984. 4th ed., 2 Vol, U.S. Army Engineer Waterways Experiment Station. Washington, DC: U.S. Government Printing Office.

Short, F. T. 1987. Effects of sediment nutrients on seagrasses: Literature review and mesocosm experiment. *Aquatic Botany* 27:41-57.

Sjøtun, K., and S. Fredriksen. 1995. Growth allocation in *Laminaria hyperborea* in relation to age and wave exposure. *Marine Ecology Progress Series* 126:213-222.

Smith, J. M. 2002. Wave pressure gauge analysis with a current. *Journal of Waterway, Port, Coastal and Ocean Engineering* 128:271-275.

Stevens, C. L., and C. H. Hurd. 1997. Boundary-layers around bladed aquatic macrophytes. *Hydrobiologia* 346:119-128.

Svendsen, I. A., K. Haas, and Q. Zhao. 2000. *Quasi-3D nearshore circulation model, SHORECIRC, Version 1.3.6*. Report, Center for Applied Coastal Research. University of Delaware, Newark.

Teeter, A. M., B. H. Johnson, C. Berger, G. Stelling, N. W. Scheffner, M. H. Garcia, and T. M. Parchure. 2001. Hydrodynamic and sediment transport modeling with emphasis on shallow-water, vegetated areas (lakes, reservoirs, estuaries and lagoons). *Hydrobiologia* 444: 1-24.

Teeter, A. M. 2001. *Sediment resuspension and circulation of dredged material in Laguna Madre, Texas*. Technical Report. Vicksburg, MS: U.S. Army Engineer Research and Development Center.

Thomas, F. I. M., C. D. Cornelisen, and J. M. Zande. 2000. Effects of water velocity and canopy morphology on ammonium uptake by seagrass communities. *Ecology* 81:2704-2713.

U.S. Army Corps of Engineers. 2002. *Coastal Engineering Manual.* Engineer Manual 1110-2-1100, U.S. Army Corps of Engineers, Washington, D.C. (in 6 volumes).

van Katwijk, M. M., and D. C. R. Hermus. 2000. Effects of water dynamics on *Zostera marina*: Transplantation experiments in the intertidal Dutch Wadden Sea. *Marine Ecology Progress Series* 208:107-118.

van Katwijk, M. M. 2000. *Possibilities for restoration of* Zostera marina *beds in the Dutch Wadden Sea*. PhD thesis, University of Nijmegen, The Netherlands. 160 pp.

van Keulen, M., and M. A. Borowitzka. 2002. Comparison of water velocity profiles through dissimilar seagrasses measured with a simple and inexpensive current meter. *Bulletin of Marine Science* 71:1257-1267.

van Keulen, M., E. I. Paling, and C. J. Walker. 2003. Effect of planting unit size and sediment stabilization on seagrass transplants in Western Australia. *Restoration Ecology* 11:50-55.

Verduin, J. J., and J. O. Backhaus. 2000. Dynamics of plant-flow interactions for the seagrass *Amphibolis antarctica*: Field observations and model simulations. *Estuarine Coastal and Shelf Science* 50:185-204.

Verhagen, H.J. and M. van der Wegen. 1998. User manual CRESS: coastal and river engineering support system. In *Dikes and revetments: design maintenance and safety assessment*. K. W. Pilarczyk, ed., 525 – 536. AA Balkema, Rotterdam.

Wallace, S., and R. Cox. 1997. Seagrass and wave hydrodynamics. *Pacific Coasts and Ports '97: Proceedings of the 13th Australasian Coastal and Ocean Engineering Conference and the 6th Australasian Port and Harbour Conference, Christchurch, New Zealand*, 69-73.

Walker, D. I., T. J. B. Carruthers, P. F. Morrison, and A. J. McComb. 1996. Experimental manipulation of canopy density in a temperate seagrass [*Amphibolis griffithii* (Black) den Hartog] meadow: Effects on sediments, p. 117-122. In: *Seagrass biology. Proceedings of an International Workshop, Faculty of Sciences, University of Western Australia, Perth.* : J. Kuo, R. C. Phillips, D. I. Walker, and H. Kirkman, ed.

Wanless, H. R. 1981. Fining upwards sedimentary sequences generated in seagrass beds. *Journal of Sedimentary Petrology* 51:445-454.

Ward, L. G., W. M. Kemp, and W. E. Boynton. 1984. The influence of waves and seagrass communities on suspended particulates in an estuarine embayment. *Marine Geology* 59:85-103.

Wilcock, P. R., D. S. Miller, R. H. Shea, and R. T. Kerkin. 1998. Frequency of effective wave activity and the recession of coastal bluffs: Calvert Cliffs, Maryland. *Journal of Coastal Research* 14: 256-268.

Wyllie-Echeverria, S., K. J. Paruelo, Gunnarsson, M. A. Mateo, J. A. Borg, P. Renom, J. Kuo, A. Schanz, F. Hellblom, E. Jackson, G. Pergent, C. Pergent-Martini, M. Johnson, J. Sanchez-Lizaso, C. F. Boudouresque, and K. Aioi. 2002. Protecting the seagrass biome: Report from the traditional seagrass knowledge working group. *Bulletin of Marine Science* 71: 1415-1417.

Wing, S. R., J. J. Leichter, and M. W. Denny. 1993. A dynamaic model for wave-induced light fluctuations in a kelp forest. *Limnology and Oceanography* 38(2): 396-407.

Wing, S. R., and M. R. Patterson. 1993. Effects of wave-induced lightflecks in the intertidal zone on photosynthesis in the macroalgae *Postelsia palmaeformis* and *Hedophyllum sessile*. *Marine Biology* 116: 519-525.

Appendix: Glossary of Terms

Acclimation	Process by which plants and animals physiologically adapt to environmental conditions. It differs from 'adaptation' in that it does not involve genetics.
Acoustic Doppler Current Profiler	An instrument that uses the Doppler shift of reflected sound from projected acoustic beams to measure profiles of velocity, usually from just above the bottom to just below the surface.
Advection	The transport of a dissolved or suspended quantity by flowing water (here it refers to horizontal transport of sediments by currents).
Algae	Aquatic plants (freshwater to marine) that reproduce via spores. Algae can be composed of a single cell or reach 25 m in length (kelp). Also see 'Macroalgae,' Phytoplankton' and 'seaweed.'
Bathymetry	The spatial distribution of bottom depth in bodies of water.
Biomass	Weight of biological material (plants or animals) expressed as a function of area or volume.
Bottom roughness coefficient	Within the bottom boundary layer, the value of the 0 flow speed intercept height on a plot of flow speed against the logarithm of height above bottom. In rough turbulent flow, the bottom roughness coefficient is equal to the physical bottom roughness divided by 30. A larger roughness coefficient means higher drag on flow, given the same flow speed.
Bottom shear stress	The force per unit area acting on the bottom due to strong vertical gradients (shear) in the fluid immediately above the bottom. Bottom shear stress is often computed as a drag coefficient multiplied by velocity (at a defined height) squared.
Bottom sheltering	Protection of the bottom from fluid forces, caused by the form drag of obstacles such as seagrasses and/or the deflection of flow away from the bottom.
Boundary layer	The layer of reduced velocity that is immediately adjacent to the surface of a solid past which the water is flowing.
Breaking zone	The nearshore zone in which wave heights decrease rapidly and turbulence levels increase markedly due to wave breaking.
Breakwater	A barrier that protects the shoreline from the full impact of waves
Canopy height	Height above the sediment to which most (2/3) of the seagrass leaves grow (see Figure 2).
Chop or wind-sea	Short, steep water waves of higher frequency generated locally by the wind, with a broad distribution of wavelengths/periods.
Cohesive sediment	Sediments composed of clay, silt, and/or organic matter for which the dominant stabilizing force is the tendency of particles to stick together, rather than the weight of the particles.

Consolidation	The process by which a sediment layer decreases in height due to the expulsion of water. Consolidation often occurs when the weight of a sediment layer squeezes the water out of the space between sediment particles.
Crest	The highest point of a wave cycle.
Curvilinear	Describes a coordinate system that bends to follow the shape of the bottom or coastline, as opposed to a Cartesian coordinate system with only rectulangular cells.
Diatom	Single celled phytoplankton with an external skeleton of silica.
Diffusive boundary layer	Sublayer of the boundary layer where the flux of molecules occurs via diffusion.
Directional wave spectrum	The distribution of wave energy as a function of both wave frequency (period^{-1}) and wave direction (usually the direction from which the waves are coming).
DIWASP	A DIrectional WAve SPectra toolbox for MATLAB.
Drag coefficient	The ratio between fluid drag and the product of fluid density and velocity squared, for flow over a boundary or around an obstacle; a higher drag coefficient means greater drag for the same velocity.
Duration	The amount of time for which a given wind has been blowing.
Ecosystem engineer	An organism that has the capacity to alter the environment it inhabits.
Ecosystem service	Goods provided by natural communities (e.g. the capacity of seagrasses to remove nutrients from the water column).
Ebb	Outflow of the tide.
Electromagnetic velocity sensor	An instrument that measures components of water velocity at a fixed point in space by sensing flow-induced changes in an emitted electromagnetic field.
Energy dissipation	Loss of energy over time due to breaking or friction.
Epiphyte	Plants that grow on the surface of other plants. In the case of seagrasses, algae that grow on seagrass leaves and host a community of associated bacteria and grazers.
Erosion rate	The rate at which sediment is eroded (or resuspended) from the bottom.
Euphotic zone	Surface waters that receive sufficient light to support photosynthesis (1 percent of surface light).
Fetch	The length of water over which a given wind has blown.
Fine particles	Particles with sediment grain size smaller than 63 μm (silt and clay).
Flood	Inflow of the tide.
Flow speed	The rate of motion of a fluid.
Flux boundary condition	A type of model boundary condition in which the time-dependent fluid volume flux (flow speed times cross-sectional area) across the boundary is specified.

Form drag	Frictional force that arises from the form of an object, in addition to the drag of its surface. Form drag is primarily due to flow separation and turbulence behind the object.
Free-stream velocity	A reference velocity away from the region of boundary or object influence. Here it refers to the axial velocity in a flume measured upstream of the leading edge of a seagrass bed (so not influenced by the seagrass).
Frictional damping	Momentum or energy loss due to friction.
Frictional drag	Force that opposes fluid motion due to flow over a boundary or around an obstacle.
Geomorphology	Description of the nature and history of the landforms and the processes that create them.
Group velocity	The rate at which wave energy propagates through space.
Habitat	The place inhabited by a plant or animal.
Heaviside step function	In the present context, a function defined to be 0 for all arguments less than 0, and 1 for all arguments greater than or equal to 0.
Infragravity wave	Long waves with periods of 30 sec to several minutes, usually generated by interactions between wave refraction/breaking and nearshore bathymetry, propagating alongshore rather than across-shore.
Kelp	A brown macroalga found in relatively cold waters that has a distinct morphology with leaves (fronds) that can reach 75 ft in length.
Kelvin- Helmholtz instabilities	Instability that occurs when shear is present within a continuous fluid or when there is sufficient velocity difference across the interface between two fluids (e.g., between the seagrass canopy and the water above it).  Source: http://www.answers.com/topic/wavecloudsduval-jpg.
Kinematic viscosity	Measure of the resistance of a fluid to shear deformation under an applied force, normalized by fluid density.
Light-fleck	Pulse or speck of light. In seagrass habitats, light-flecks are the result of light focusing by the crest of waves in shallow wate.r
Linear or airy wave approximation	An approximation assuming that wave amplitude is small, which greatly simplifies the equations of wave motion.

Macroalga	Large (visible to the naked eye) aquatic plant (freshwater to marine) that reproduces via spores and has a relatively simple morphology: no roots, rhizomes or flowers (also referred to as 'seaweed'). Found on rocky substrates.
MATLAB	A high-level numerical computing environment and programming language created by The MathWorks, Inc., Natick, Massachusetts.
Microalga	Small (unicellular or clusters of cells) aquatic plant (freshwater to marine).
Model domain	The equivalent physical space of a model simulation. Here, the model domain is a rectangular area 720m x 5400 m.
Monochromatic	Having a single wavelength or wave period.
Nearshore	The zone that extends from the shoreline to a position marking the start of the offshore zone, typically at water depths of approximately 3-5 m.
Organic content	Amount of organic matter found in sediments. Often determined as the fraction of the sediment that is combustible at 450 ^{o}C.
Oscillatory flow	The back-and-forth motion of a fluid under waves.
Period	The time for one complete cycle of a wave to pass by a fixed point in space.
Phase speed	The rate at which a wave pattern propagates through space.
Photosynthesis	Process by which plants transform carbon dioxide, solar energy and water into chemical energy needed for growth.
Phytoplankton	Microscopic algae found in the euphotic zone.
Pressure	The force per unit area applied on a surface in a direction perpendicular to that surface.
Productivity	The rate at which a given quantity of organic material is produced by organisms such as seagrasses.
Recruitment	The addition of new individuals to a population.
REF/DIF	A model for ocean surface wave propagation that accounts for wave bending when waves travel through an area with changing depths (refraction) and wave scattering behind obstacles (diffraction). It was developed at the University of Delaware.
Resuspension	The process whereby previously deposited sediment particles are lifted back into the water column by fluid (or biogenic) forces.
Reynolds number	The ratio of inertial to viscous force in a fluid flow; low Reynolds numbers correspond to laminar flow (smooth, steady streamlines) while high Reynolds numbers correspond to turbulent flow (smooth average streamlines, but chaotic instantaneous flow).
Rhizome	Horizontal structure of seagrasses that connects shoots and roots.
Rough turbulent flow	A fully turbulent flow, such that increasing the Reynolds number does not change the qualitative behavior of the turbulence. This means that molecular viscosity no longer plays a role; for example, in rough turbulent boundary layer flow there is no viscous sublayer just above the boundary.

Roughness	Measurement of the small-scale variations in the height of a surface. Higher bottom roughness often means larger fluid drag and total bottom stress.
Sandbar	Submerged (or partly submerged) ridge of sand along a shore.
Sand wave	Large regular alterations of sand ridges (crests and troughs) which move when current velocities exceed 47 to 60 cm/sec causing a succession of depositional and erosional events at a fixed point.
SAV	See 'submersed aquatic vegetation.'
Scour	Preferential local erosion of bottom sediment due to focused currents, waves, or turbulence.
Sea-surface elevation	The height of the sea-surface with respect to a fixed reference height such as mean sea-level.
Sea-surface slope	The inclination of the sea-surface from a perfectly horizontal line.
Sea-surface vertical acceleration	Rate of change of the sea-surface vertical velocity.
Sea-surface vertical velocity	Velocity component of the sea-surface in the vertical direction.
Seagrass	Flowering marine plant.
Seaweed	See 'macroalgae.'
Sediment deposition	The process whereby sediments in the water column sink to the bottom and attach to it.
Sediment dynamics	The study of the effects of physical (and sometimes biological) forces on the motion of sediments.
Sediment grain size	Characteristic physical dimension of sediment particles. For example, a grain size for fine sand might be 0.2 mm.
Sediment transport	The motion of sediment in a flowing fluid, often separated into suspended transport and bedload transport. Suspended transport describes the 3-D movement of sediments that stay in the water column; Bed-load transport describes the rolling and hopping of sediment particles across the bottom.
Self-shading	Process of one part of the plant shading the same plant (e.g. when a seagrass leaf bends over it shades the leaf underneath).
Semidiurnal	Occurring approximately once every 12 hr.
Separation	When a flow streamline detaches from the surface of an object, such that the mean flow beyond that point is zero or recirculating. Flow beyond the point of separation is dominated by turbulence, so early flow separation usually means higher drag.
Shallow water wave	Waves for which the local water depth is less than 5% of the wavelength.
Shear velocity	The main scale velocity for boundary layer turbulence, defined as the square root of bottom shear stress divided by fluid density.
Shoaling	Changes in wave height and wavelength as waves propagate into shallower water.

Shoot	Cluster of leaves (see Figure 1).
SHORECIRC	A numerical nearshore circulation model that accounts for currents induced by wave breaking, as well as other more conventional forces. SHORECIRC was developed at the University of Delaware.
Sill	Submersed breakwater.
Skin friction	Frictional force that arises from shear stresses generated at the surface of an object or at the bottom of a water column. Skin friction is the force that most directly dislodges sediment particles or controls interfacial fluxes.
Steady current	Flow speed that doesn't change with time.
Submersed aquatic vegetation (SAV)	Flowering plants growing submersed in habitats covering a wide range of salinities, from freshwater to marine. Note that seagrasses can also be referred to as SAV.
Surface gravity wave	Waves traveling on the free surface of a fluid medium and having a restoring force of gravity or buoyancy.
Suspended sediment concentration	The mass of suspended sediment in a unit volume of water.
Swells	Long period, long crested surface waves generated far away and propagating into a region of interest.
Tidal current	Oscillatory velocity induced by the surface tide, with flood corresponding to the incoming tide and ebb corresponding to the outgoing tide.
Transect	A reference line drawn through a domain of interest. Here it refers to a slice that is perpendicular to the shoreline.
Trough	The lowest point of a wave cycle.
Turbulent wake interference	Occurs when the turbulent wake of an upstream object encounters a downstream object.
Vector addition	Summation of two vectors by the addition of their directional components; for example, adding two east components of velocity and two north components of velocity to calculate the total velocity vector.
Von Karman constant	The constant of proportionality between shear velocity and the product of height and velocity shear at any height z in the constant stress region of a turbulent boundary layer. It was determined experimentally to have a value of 0.4.
Wave	A disturbance that propagates through space, transmitting energy but relatively little mass.
Wave energy attenuation	Decrease in wave energy, as the wave propagates due to frictional forces or spreading of wave energy, or with depth below the surface for deep water or intermediate waves.
Wave energy flux or wave power	The product of wave energy and wave group velocity. When wave power is dissipated by bottom friction or breaking, the wave power lost is equal to the work done by the waves on the bottom and/or shoreline.

REPORT DOCUMENTATION PAGE

Form Approved
OMB No. 0704-0188

1. REPORT DATE *(DD-MM-YYYY)*	2. REPORT TYPE	3. DATES COVERED *(From - To)*
November 2006	Final report	

4. TITLE AND SUBTITLE

Waves in Seagrass Systems: Review and Technical Recommendations

5a. CONTRACT NUMBER

5b. GRANT NUMBER

5c. PROGRAM ELEMENT NUMBER

6. AUTHOR(S)

Evamaria W. Koch, Larry P. Sanford, Shih-Nan Chen, Deborah J. Shafer, and Jane McKee Smith

5d. PROJECT NUMBER

5e. TASK NUMBER

5f. WORK UNIT NUMBER
122687

7. PERFORMING ORGANIZATION NAME(S) AND ADDRESS(ES)

Horn Point Laboratory, University of Maryland Center for Environmental Science, P.O. Box 775, Cambridge, MD 21613;
U.S. Army Engineer Research and Development Center, Environmental Laboratory, 3909 Halls Ferry Road, Vicksburg, MS 39180-6199;
U.S. Army Engineer Research and Development Center, Coastal and Hydraulics Laboratory, 3909 Halls Ferry Road, Vicksburg, MS 39180-6199

8. PERFORMING ORGANIZATION REPORT NUMBER

ERDC TR-06-15

9. SPONSORING / MONITORING AGENCY NAME(S) AND ADDRESS(ES)

U.S. Army Corps of Engineers
Washington, DC 20314-1000

10. SPONSOR/MONITOR'S ACRONYM(S)

11. SPONSOR/MONITOR'S REPORT NUMBER(S)

12. DISTRIBUTION / AVAILABILITY STATEMENT

Available for public release; distribution unlimited.

13. SUPPLEMENTARY NOTES

14. ABSTRACT

Seagrasses are rooted flowering marine plants that provide a variety of ecosystem services to the coastal areas they colonize. Attenuation of currents and waves and sediment stabilization are often listed among these services. Although we have a reasonably good understanding of how currents affect seagrasses and vice-versa, less is known about interactions between waves and seagrasses, and standard methods for research on waves in seagrass systems have not yet been established. This report presents background information needed to inform and encourage further studies on waves in seagrass systems from both field and modeling perspectives. It reviews current knowledge of waves in seagrass systems, encompassing field and laboratory data as well as modeling efforts. It then describes various methods for measuring waves in seagrass colonized areas and modeling the dynamics of wave-seagrass interactions. Standardization of experimental designs, instrumentation, analyses, and modeling approaches to allow for ready comparison between studies is encouraged.

15. SUBJECT TERMS

Seagrass	Wave attenuation	Ecosystem
Waves	Wave measurement	Submerged aquatic vegetation
	Wave-seagrass interaction	Seagrass terminology

16. SECURITY CLASSIFICATION OF:			17. LIMITATION OF ABSTRACT	18. NUMBER OF PAGES	19a. NAME OF RESPONSIBLE PERSON
a. REPORT	b. ABSTRACT	c. THIS PAGE			19b. TELEPHONE NUMBER *(include area code)*
UNCLASSIFIED	UNCLASSIFIED	UNCLASSIFIED		92	